Calibration in Paris:
Method and results

L. Rolland

L.P.N.H.E. Paris 6/7 - 4,Place Jussieu - 75252 Paris Cedex 05 - France

December 2003

Contents

1 Introduction

The calibration of the H.E.S.S. cameras is necessary before any analysis. In this note, the calibrated parameters are described. Then the methods used in Paris to get the calibration information from the runs are described. The information are stored in a database and files.

The calibration is done after each shift period in Namibia, when the data are back in Europe. Generally, the three weeks of shift correspond to a calibration period. Nevertheless, it can be divided into more periods if the camera configuration has been changed during the shift period.

After one year of acquisition, the calibration has highlighted characteristics of the first two cameras. The results are commented on at the end of the note.

2 Calibration parameters

In this section, the parameters that need to be calibrated are described. Some of them, such as the gains, the pedestals and the detection of the non-noperational pixels are necessary for the data analysis. The flat-field coefficients are used to improve the precision of the analysis. Some current baselines (HVI and DCI) are used to estimate the night sky background (NSB) in the data.

2.1 Drawer temperature

The temperature of each drawer of the camera is controlled at three points:

- T1 is measured at the rear of the drawer, in a poorly ventilated zone ;
- T2 is measured near the Analogue Ring Samplers (ARS) ;
- T3 is measured at the rear of the upper photo-multiplier tubes (PMTs), near the DC / DC converters.

The online monitoring of the temperature is used to switch off the cameras if the temperature is too high ($> 55°\mathrm{C}$).

The temperature is used offline to determine the evolution of the calibration parameters with the temperature. The section 4.2 gives the evolution of the calibration parameters with the temperature. These results imply that the temperature must thus be very stable during the calibration runs.

2.2 Photo-multiplier dark currents

Two methods are used to measure the dark current of each pixel of the H.E.S.S. cameras. The causes of the dark current are first described. We will see that it shifts when the PMT is illuminated. Then, each measurement of the dark current, HVI and DCI, is described. This highlights some specific features of each of them.

2.2.1 The dark current

The current that flows into the anode circuit when the voltage is applied to the PMT in total darkness has two components. One is a continuous current due to leakage on glass and surfaces, the other is intermittent, consisting of pulses.

The causes of the dark current are mainly:

- leakage current
- thermionic emission
- field emission

- background radiation

Each of them is now described.

Leakage currents They are the unique cause of the continuous component of the dark current. They are due to the surface conductivity of the PMT components (electrode supports, envelope, base). The leakage currents vary linearly with the high voltage applied. It is not strongly correlated with the temperature.

Thermionic emission At low voltage, it is the main cause of the pulsed component of the dark current. Electrons are emitted by the cathode or by the dynodes. They are then accelerated towards the other dynodes and create a cascade of electrons in the PMT. A signal is thus measured at the anode. Dark pulses due to the thermoinic emission of the photo-cathode are mainly of the single photo-electron type and those originating from the dynodes are amplified less. This emission decreases rapidly as temperature decreases.

Field emission Although the electric fields in a PMT are low, there is some emission due to one field effect because of inevitable roughness of the electrodes. It is an additional cause of the pulsed component of the dark current. The pulse rate due to field emission does not depend much on temperature. It depends on the high voltage and is the main component of the dark current at high voltages.

Background radiation Background radiation is another cause of dark pulses. High energy charged particles (from cosmic rays or radioactivity) can give rise to Cerenkov radiation in the tube window, which causes photo-emission. This can generate several photons at a time, so the dark pulses are often of high amplitude.

Figure 1 shows the three ranges of supply voltage in which each of the causes of dark current predominates. The background radiation is negligible.

The H.E.S.S. PMTs A high voltage of about $1000\,\mathrm{V}$ is set on the PMTs: a voltage divider bridge sets the voltage between the 8 dynodes proportionally to 1,2,1,1,3,1,1,1. As the high voltage is rather low, the predominant cause of dark current is the leakage current.

Two currents are measured for each PMT. The HVI (high voltage intensity) is the current in the high voltage supply circuit. The DCI (dark current intensity) is the current in the anode circuit. Both measurements are now described more precisely. The evolution of both currents with the temperature and the light is explained.

2.2.2 HVI: High Voltage Intensity

The dark current can be measured in the high voltage generator circuit: this measurement is called the HVI.

The HVI in the dark In the dark, the HVI is mainly due to the leakage current. We have seen that this current does not vary strongly with the temperature but depends on the high voltage. Figure 2 gives the evolution of the HVI with high voltage. The 960 PMTs of the camera do not have the same high voltage, their HVI values in the dark are different: figure 2 gives the distribution of the HVI in the dark for the PMTs of the camera of CT3.

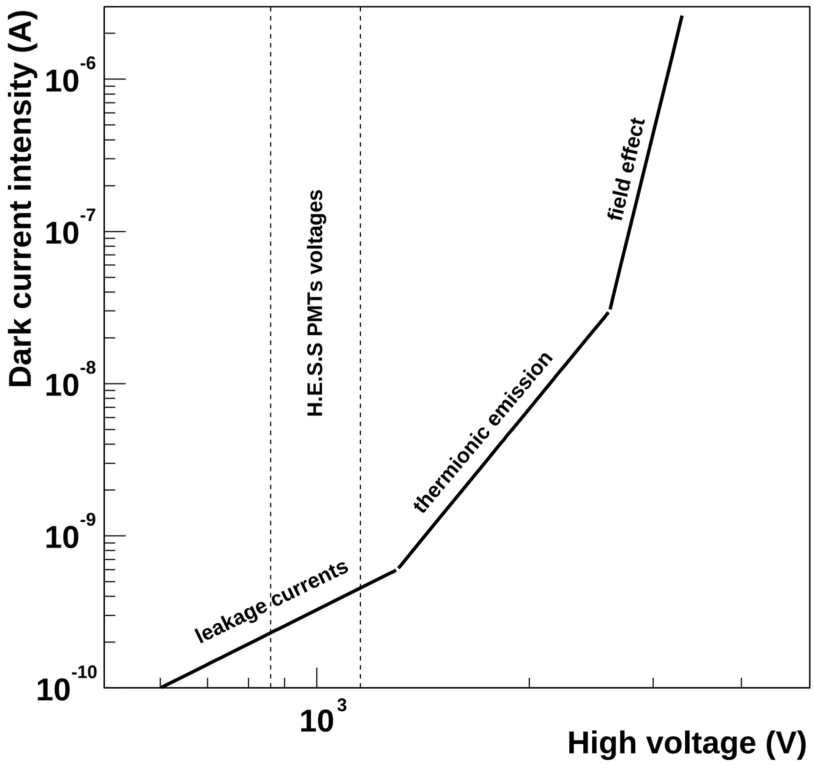

Figure 1: Three ranges of supply voltage in which the causes of dark current are predominant.

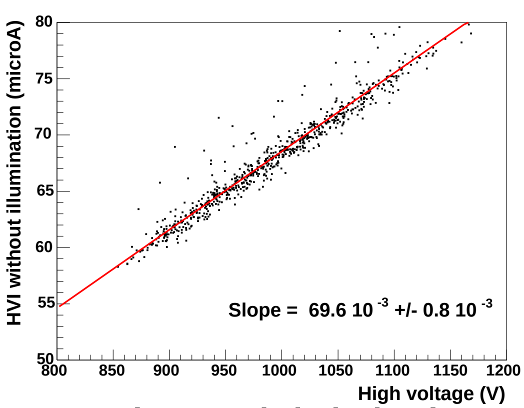

HVI evolution with the high voltage.

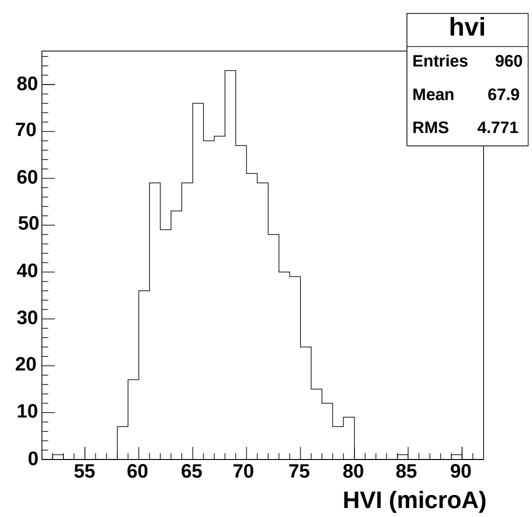

HVI distribution in the dark.

Figure 2: HVI evolution with the high voltage and HVI distribution in one camera (CT2).

The HVI with NSB When the PMT is illuminated, the photo-electrons remove electrons from the dynodes. However, the dynodes stay electrically neutral: a current coming from the high voltage generator compensates this loss of electrons. This current increases with the high voltage of the PMT (as more electrons are removed). It also increases with the light (the number of input photons increases). This last property is described in note [1]. When the HVI is measured, it is the sum of this current and of the dark current.

To conclude, the HVI can be used to estimate the NSB during the analysis of the data runs: the shift between the HVI in the dark and the HVI measured with NSB varies linearly with the NSB value (see note [1]) and has a low dependance on the temperature. To carry out this measurement, the HVI values in the dark need to be calibrated for each PMT.

2.2.3 DCI: the anode current

The DCI (Dark Current Intensity) is measured as a voltage across a resistor at the anode of the PMT. The anode current is measured after the PMT and a chain of amplifiers with an integrator as drawn in figure 3. The duration Δt of the integration is about $5\,\mu$s. The gain G of the electronic chain is about 1000.

The DCI in the dark In the dark, the main component of the DCi is the leakage current which is quite independant of temperature. Nevertheless, the electronic offsets of the amplifiers vary slightly with the temperature. As these offsets are amplified by a gain of 1000, the DCI measured in the dark is very correlated with the temperature. Moreover, the offsets are slightly different from a channel to another. This results in a broad distribution of the DCI values in the dark as shown in figure 4.

The DCI with NSB When the PMT is illuminated, the photo-electron pulses are added to the dark current at the anode of the PMT. The dependance of the added current on the NSB is now shown.

As a PMT has a nominal gain of the order of 2×10^5, a photo-electron will give at the anode a pulse of ADC count $Q_e = 2 \times 10^5 \times 1.6 \times 10^{-19}\,\mathrm{C} = 32\,\mathrm{fC}$. The pulse half-width is about $3\,\mathrm{ns}$, negligible compared to the integration duration. The current is converted into a voltage V_{DCI} using a resistor $\mathrm{R} = 50\,\Omega$.

If we consider an input rate f, there are $N = f \times \Delta t$ pulses in the $5\,\mu$s of integration. The total charge is then $N \times Q_e$. This charge is spread over the integration duration and measured at the pins of the resistor R. The voltage measured after the amplification G is then:

$$V_{\mathrm{DCI}} = \mathrm{G} \times \mathrm{R} \times \frac{\mathrm{N} \times \mathrm{Q_e}}{\Delta \mathrm{t}} = \mathrm{G} \times \mathrm{R} \times \mathrm{f} \times \mathrm{Q_e}$$

The voltage V_{DCI} is added to the value of the DCI in the dark. For an input rate of $10\,\mathrm{MHz}$, we obtain $V_{\mathrm{DCI}} = 16\,\mathrm{mV}$, and for $100\,\mathrm{MHz}$ $V_{DCI} = 160\,\mathrm{mV}$. These values are very close to the DCI shifts that are measured in the cameras: table 1 gives some results from note [1].

To conclude, if the evolutions of the DCI with the temperature are known and the temperatures measured, the DCI shift can be used to measure the NSB received by each pixel during the acquisitions in Namibia. We thus need to know the DCI value in the dark depending on the temperature: this is the aim of the DCI calibration.

2.3 The acquisition channel

Each drawer (16 pixels) is composed of two acquisition cards reading the data from 8 PMTs, as shown in s figure 5. For each pixel, there are three channels, one trigger channel and two acquisition channels with different gains: the high-gain channel is used to detect low signals from 1 to 200 photo-electrons; The low-gain channel is used to have a high dynamic range from 15 to 1600 photo-electrons. The PMT signal is measured across a resistor R_{PM} and amplified into the two acquisition channels, low gain

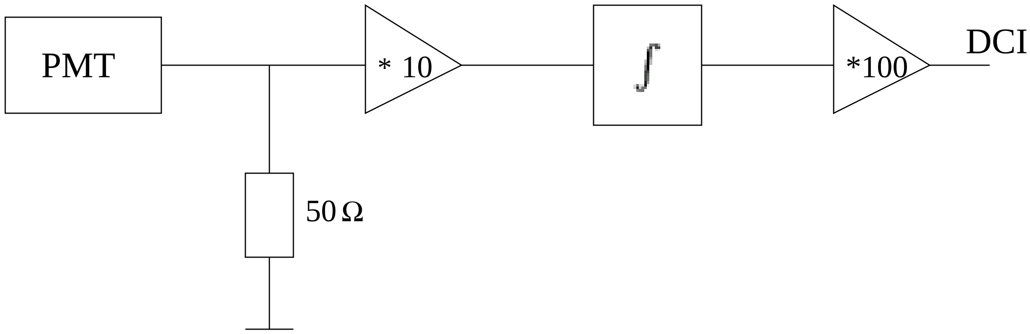

Figure 3: Electronic chain for the measurement of the DCI value.

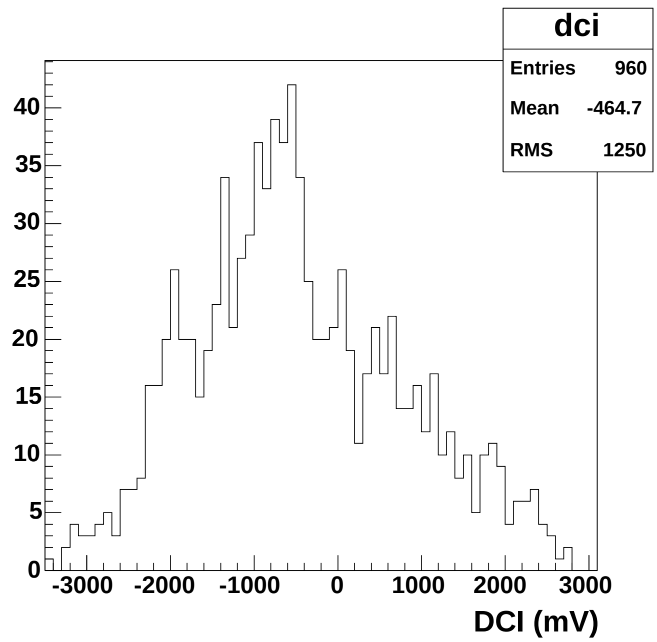

Figure 4: DCI distribution in the dark (the mean temperature is $14°\mathrm{C}$).

NSB frequency (Hz)	DCI shift (mV)
$\sim 1 \times 10^7$	17.7
$\sim 5 \times 10^7$	88.3
$\sim 1 \times 10^8$	177.

Table 1: Experimental DCI shift values for different illumination intensities

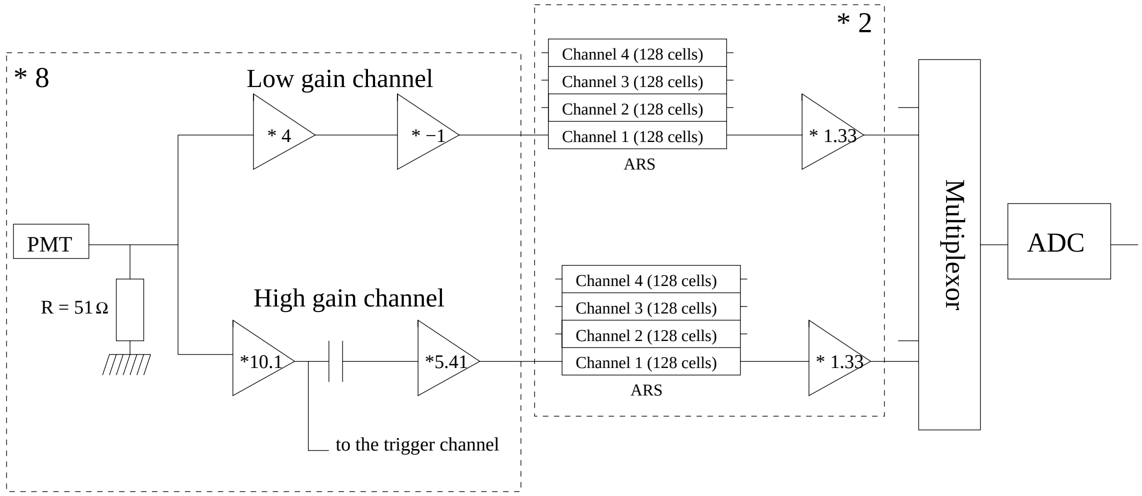

Figure 5: Acquisition channels scheme for one acquisition card (8 PMTs).

G^{LG} and high gain G^{HG}. The analogue signal is then sampled into an ARS of 128 cells of 1 ns. Only N_L cells (16) are read: the analogue signal of these cells is amplified to adapt the signal range and a multiplexor distributes the signal from 4 ARSs (8 PMTs) into one Analogue to Digital Convertor (ADC) with a conversion factor V_{ADC} of 1.22 mV / ADC step. In charge mode, the N_L samples are summed and give the ADC count read by the pixel.
The base-lines for both channels at the input of the ADC are of the order of -0.9 V, which are converted into -730 ADC counts. In charge mode, after the summation of the 16 samples, the ADC counts are then of the order of -11500 ADC counts: this is the electronic pedestal position. The noise at the input of the ADC is about 20 mV in the high-gain channel, which gives a pedestal RMS of 16 ADC counts, and 7 mV in the low-gain channel, which gives a pedestal RMS of 6 ADC counts.
When the PMT receives some photo-electrons, the ADC count is higher than the electronic pedestal position. The distance between the ADC count and the electronic pedestal position is proportional to the light intensity received by the PMT.

2.4 The pedestals

The pedestal is the ADC count measured after the ADC when the pixel does not receive any Cerenkov pulses: to get a pedestal charge histogram, we need a random trigger. Note that what we call “charge histograms” are filled with ADC counts and not with the charges in photo-electrons. For the calibration, there are two types of pedestals.

The pedestal in the dark The **electronic pedestal** of a channel is the charge histogram measured in the dark after the ADC, with a random trigger. Electronic noise results in some fluctuations of the pedestal value: the ADC count distribution in the dark is a Gaussian whose mean is the electronic pedestal position (about -11500 ADC counts) and whose width is a measurement of the electronic noise of the channel. It is very important to determine the electronic pedestal position precisely because it is the value to be substacted to obtain the physical signal (the charge) measured by the PMT in the data runs.

The pedestal with NSB The **run pedestal** is the charge histogram measured with a low intensity ligh background (i.e., during the data taking). As there is a RC circuit and a gain -1 at the output of the PMTs, the short photo-electron pulses (positive) are followed by a slightly negative signal over

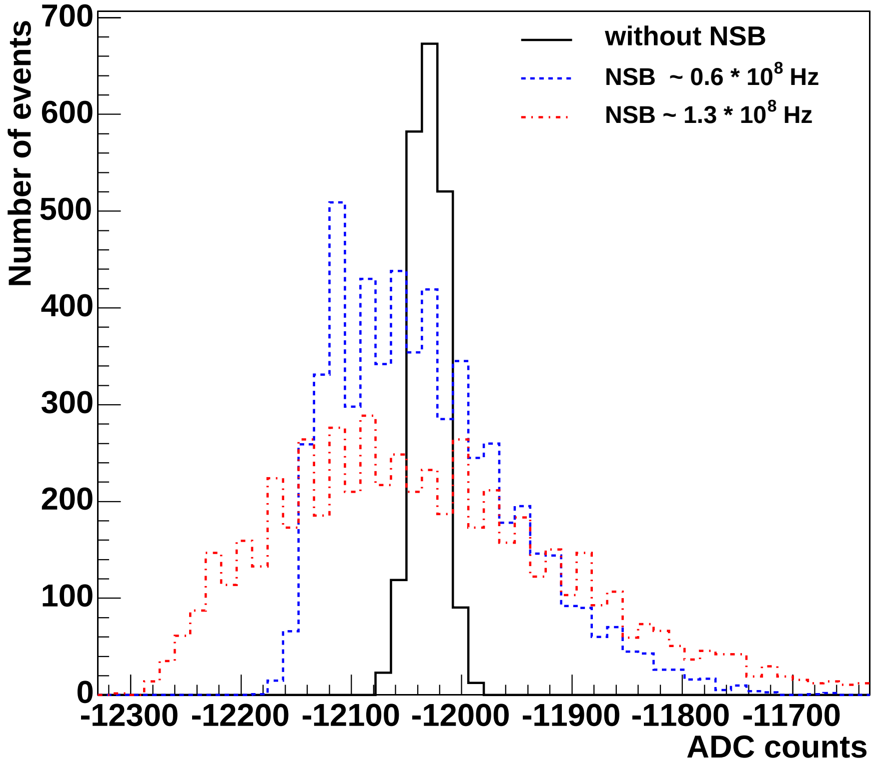

Figure 6: Pedestal variations with the NSB value in different data runs: the mean is constant, but the zero photo-electron peak is translated towards negative values and the distribution is widened when the NSB increases.

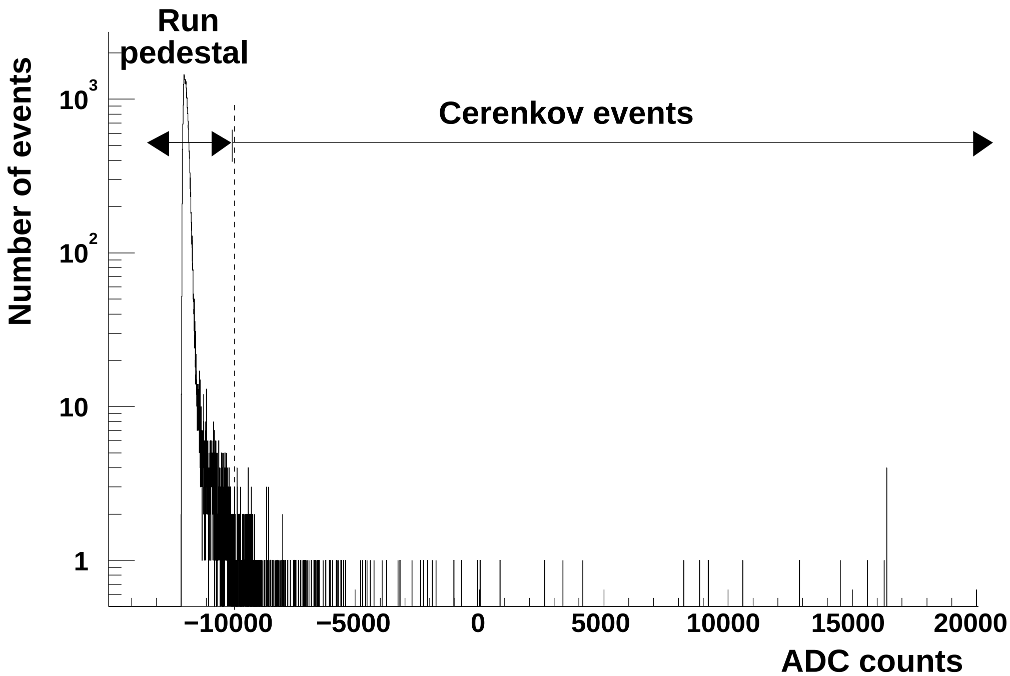

Figure 7: Charge histogram of a pixel in a data run: the run pedestal is clearly visible, and the Cerenkov events give some high charge events.

a few micro-seconds. During this time, the PMT can receive other NSB events, each of them will introduce a new shift of the baseline. Random $16\,\mathrm{ns}$ windows are sampled, digitized and summed to get the ADC counts of the pixels. Two cases can happen. In the first case, the window does not integrate any photo-electron pulse, but only the shifted base line: the ADC count is then lower than in the dark. In the second case, the window integrates a part of a photo-electron pulse.The run pedestal histogram thus has two components: the zero photo-electron peak shifted towards the left when the NSB increases, and the events with photo-electrons pulses shifted towards the right. When the NSB is higher than $3 \times 10^8\,\mathrm{Hz}$, a part of an NSB photo-electron pulse is always in the readout window: the zero photo-electron peak disappears and the entire pedestal histogram moves toward the right. Figure 6 shows the evolution of the pedestal shape with the NSB. In note [2], it is shown that when the NSB is lower than 3×10^8 Hz (0.3×10^9 photo-electrons /s), the mean of the run pedestal histogram is the electronic pedestal position. In Namibia, the mean NSB value is 10^8 Hz: the pedestal position can thus be defined as the mean of the run pedestal histogram. Hereafter, the mean of the electronic pedestal histogram and the mean of the run pedestal charge histogram will be called **pedestal position**. Note than if the NSB is higher than 2×10^8 Hz, the pedestal position is the mean of the run pedestal histogram and can be higher than the electronic pedestal position.

Using the zero photo-electron peak position, the measured charge for an event is the sum of two components: the Cerenkov and the NSB charges. Using the pedestal position, the measured charge for an event is only composed of the Cerenkov charge. For the analysis of the Cerenkov events, we use the pedestal position only.

A standard ADC count distribution is shown in figure 7. Two components are visible:

- the NSB events: the run pedestal histogram
- the Cerenkov events: the high charge events

As the pedestal positions vary with the temperature (see section 4.2), they are calculated very regularly (every 2 minutes) in the data runs (see section 3.4). The charge of each pixel can then be calculated for each event.

2.5 Gains in high and low-gain channels

The PMT signal is measured across a resistor $R_{\rm PM}$ and amplified into two acquisition channels, low gain $G^{\rm LG}$ and high gain $G^{\rm HG}$ (figure 5). The analogue signal is then converted into a numeric signal of $N_{\rm L}$ (16) samples of 1 ns: the 16 ns read-out window is set so that the pulse of the PMT is in (see figure 10 and note [1]). In charge mode, these $N_{\rm L}$ values are summed. We call $V_{\rm ADC}$ the conversion factor of the ADC (1.22 mV / ADC step).

When one photo-electron of charge e is emitted by the photocathode, $G_{\rm PM}$ electrons are obtained at the anode of the PMT. As we integrate the signal over $N_{\rm L}$ ns, we can consider the current-voltage conversion of the resistor is:

$$V_{\rm PM} \;=\; R_{\rm PM} \times \frac{G_{\rm PM} \times e}{N_{\rm L}(\rm ns)}$$

The voltage is then amplified by a factor G ($G^{\rm HG}$ or $G^{\rm LG}$), and converted by the ADC with a conversion factor $V_{\rm ADC}$ of 1.22 mV / ADC step. The number of ADC counts for one photo-electron in the input of the channel is thus:

$$\gamma_e^{\rm ADC} \;=V_{\rm PM} \times G \times V_{\rm ADC}$$

We define the gain as this conversion factor: it is the **number of ADC counts per photo-electron**.

The gain is a property of the entire acquisition channel: it takes into account the PMT gain $G_{\rm PM}$, the amplification gain G of the readout channel ($G^{\rm HG}$ and $G^{\rm LG}$ for high and low-gain channels), the summation of the $N_{\rm L}$ samples and the ADC conversion $V_{\rm ADC}$.

The gain discrepancy between both acquisition channels is due to the amplifiers gains: the ratio should then be of $G^{\rm HG}/G^{\rm LG} \;=\; 13.7$. As the high-voltage values of the PMTs are set in Paris testbench to have the nominal gains equal to 80 in the high-gain channels, the low gains are of the order of 5.8.

The gain is the conversion factor used during the analysis to get the charge received by a PMT from the difference between the ADC counts and the electronic pedestal position.

During the calibration, we calculate the high gains for each pixel with specific runs (see section 3.3). The low gains are calculated indirectly using the data runs: we calibrate the high-gain to low-gain ratios for each pixel (see section 3.6).

2.6 Flat-field coefficients

The flat-field coefficient of a pixel is the **inverse of the relative light-collection efficiency**: it is the ratio of the mean charge over the 960 operational pixels of the camera and the mean charge of the pixel. Thus the mean value of the flat-field coefficient distribution is 1.

It is a correction of second order, taking into account the inhomogeneities of the pixel's light collection efficiency in the calculation of the charge received by each pixel: these inhomogeneities are due to the difference of efficiency of the Winston cones and of the photo-cathodes of the PMTs. The optical collection of the photo-electrons in the first dynode can also vary slightly from one PMT to another.
The flat-field calibration is described in section 3.7.

2.7 Non-operational pixels

The 'broken pixels' have to be removed from the calibration and the analysis. Generally, they only have a specific problem during one run: they are not really broken! It is very important to detect them for each run. Various causes of non-operational pixels can be listed in the data runs:

- **disabled HV**: the HV is disabled during the entire run.

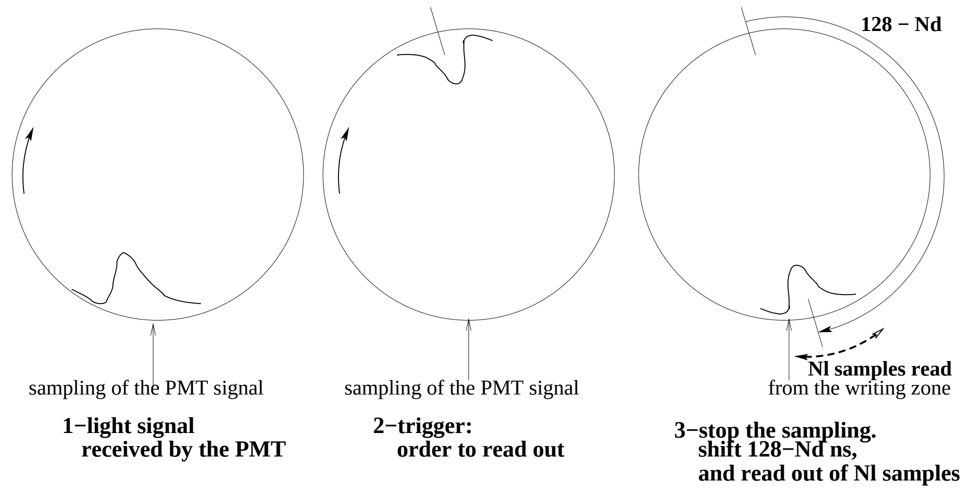

Figure 8: Readout of one channel of an ARS and definition of the parameters N_{d} and N_{L}.

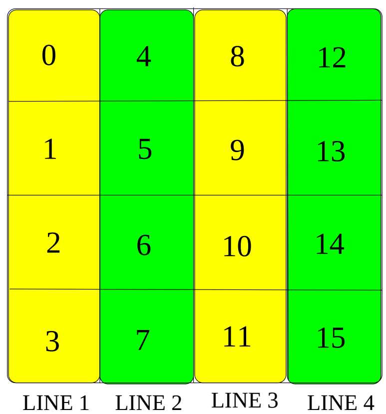

Figure 9: Correlation between PMTs-ARSs in a drawer. Each column of 4 PMTs is read by 2 ARSs: one for the low-gain channels and one for the high-gain channels.

- **unstable HV**: the HV does not have its nominal value (if the difference between its nominal HV and the monitored HV is more than 15 V or if the HV is below 700 V) or is not stable during the run (if the monitored HV dispersion (RMS) is more than 4 V). The pixels that are switched off during the run because of stars are not flagged: they are used in the calibration or the analysis until they are switched off.

- **unlocked ARS**: the way the ARS are working and the main problems they can have are described below.

- **NoSig, BadHiLo, MiscLG, MiscHG**: these described in the section 3.5.

2.7.1 The ARS in the acquisition channels

The ARS, Analogue Ring Samplers, are analogue memories used in the acquisitions channels. Their operation is described in figure 8.

To wait for the trigger signal which is formed from the signals from the 38 sectors ($\sim of 64$ pixels each)in the camera, the analogue information of each PMT has to be stored temporarily. The solution used is based on the ARS: each ARS has 4 channels of 128 cells and continuously samples the signals of 4 PMTs at 1 GHz (every nanosecond). The ARS thus keeps the history of the last 128 ns, the previous data being written over. A window of interest of N_d samples is defined: when the acquisition card

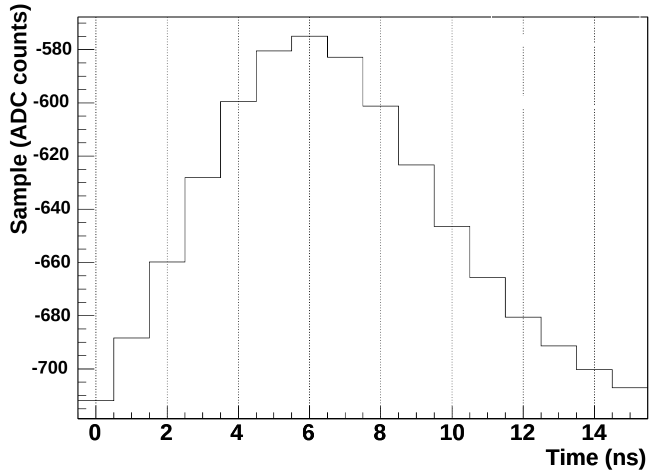

Figure 10: 16 ns sampled LED signal received by a PMT: the histogram gives the average over several sampled signals.

receives the order to read the data, the ARS stops sampling and keeps “moving” during $(128-N_d)$ ns. The readout of the data then begins: a read-out window of N_L samples is defined. In order not to lose information, N_L has to be larger than the duration of the PMT signal, but not too large in order to minimize the NSB contributions. The signal at the output of a PMT has a width of about $3\,\mathrm{ns}$ but the ARS and the amplifiers increase the width up to of the order of $10\,\mathrm{ns}$: to read the entire signal and to allow for some jitter, N_L is defined to be $16\mathrm{ns}$. N_d is the time between the moment the signal is read by the pixel and the moment the trigger signal comes back to the drawer: if N_d is too long, the signal that triggered is not yet in the readout window, but if N_d is too short, the signal that triggered has already come through the readout window and a part has been skipped. The value given to N_d is of the order of 65 samples. The precise value given to each drawer is measured in the Paris testbench (see [1]). The 16 samples from one PMT are then converted to numeric data and summed to get the ADC count of the pixel.

To summarize, the ARS are used to store the analogue signal from the PMTs during the time the trigger signal is formed and two parameters are defined to read the entire signal: the position and the width of the readout window. A mean signal sampled over a 16 ns window is shown in figure 10.

Each ARS has 4 channels. One ARS stores the data either from the high-gain channels of 4 PMTs or from the low-gain channels of 4 PMTs. The same 4 PMTs are thus read in 2 different ARS: one for the high-gain channels and one for the low-gain channels. The 4 PMTs read in one ARS form a column in the drawer as shown in figure 9. This pattern will be used to detect the unlocked ARSs. When the ARS works properly, the signals of the 4 PMTs are centred in the readout window. The ADC counts of the 4 PMTs are thus read correctly. When the ARS is unlocked, the readout windows misplaced in some proportion of the events, so for these the ADC counts are not read correctly. The main characteristics of the data read through an unlocked ARS are features present in the 4 channels read by this ARS:

- abnormal charge histograms,
- abnormal high-gain to low-gain ratios.

In the search for the unlocked ARS, the ARS is considered as unlocked if at least 2 channels out of the 4 have these features. There are different methods to find the unlocked ARS depending on the type of run. They are described below with the calibration method descriptions.

As the two acquisition channels of the pixels are read through two different ARS, there are two unlocked ARS flags: one for low-gain channel and one for high-gain channel. Thus the data from the pixel can be used if they are in the dynamic range of the operational channel.

3 Calibration methods

The calibration of the cameras is done after each shift period when the data are available in Europe. There are different steps to be performed to compute the parameters described above. The order of their computation is quite important.

In this section, the global scheme of the calibration performed in Paris is described. The calibration steps are then explained in the order they are used. The different types of run used, their selection, the methods used to compute the calibration parameters and the way they are stored are described for each step. Different methods are used to detect the unlocked ARSs: they are explained for each type of calibration run.

3.1 Global calibration scheme: databases and files

In the Paris calibration scheme, the two methods used to store the calibration information are:

- the database: the information that is stable over a period (electronic pedestals, gains, high / low ratios and flat field coefficients) are stored into a database,
- the files: the information describing a unique run (run pedestals and non-operational pixels) are stored in ROOT files.

The database scheme is the same for the four types of calibration information:

- a description of the quality of each calibration run is stored in a *run quality* table,
- the calibration information is stored for each run whose quality is correct in a *per run* table,
- the calibration information of the period, used during the analysis, is stored in a *period* table.

In the tables where the information is saved for each run, some data are always stored for each drawer as the run number, the date of the start of the run, the drawer identity and its position in the camera.

In the tables where the information is saved for a period, some information is always stored for each drawer by its identity and its position. The first and last runs of the period are also saved.

The specific calibration parameters saved in each database or files and the method used to evaluate them are described below. The table names of the database CALIBRATION are given in annexe 1. The specific software modules used to compute the calibration are given in annexe 2.

3.2 Electronic pedestal

The electronic pedestal calibration consists of the determination of the correlations of the pedestal position, the HVI and the DCI values with the temperature. They are used in the analysis to determine the night sky background for each pixel.

3.2.1 Type of run

The ElectronicPedestalRuns are performed in the dark (lid closed), in charge mode, using soft (random) triggers. The monitoring events are very important in these runs: “scaler events” to measure the DCI current, “hv events” to measure the high voltage and the HVI current and “temperature events” to measure the temperature.

These runs are used to calibrate the variations of the pedestal position, the HVI and the DCI with the temperature. The calibration parameters are saved in the CALIBRATION database.

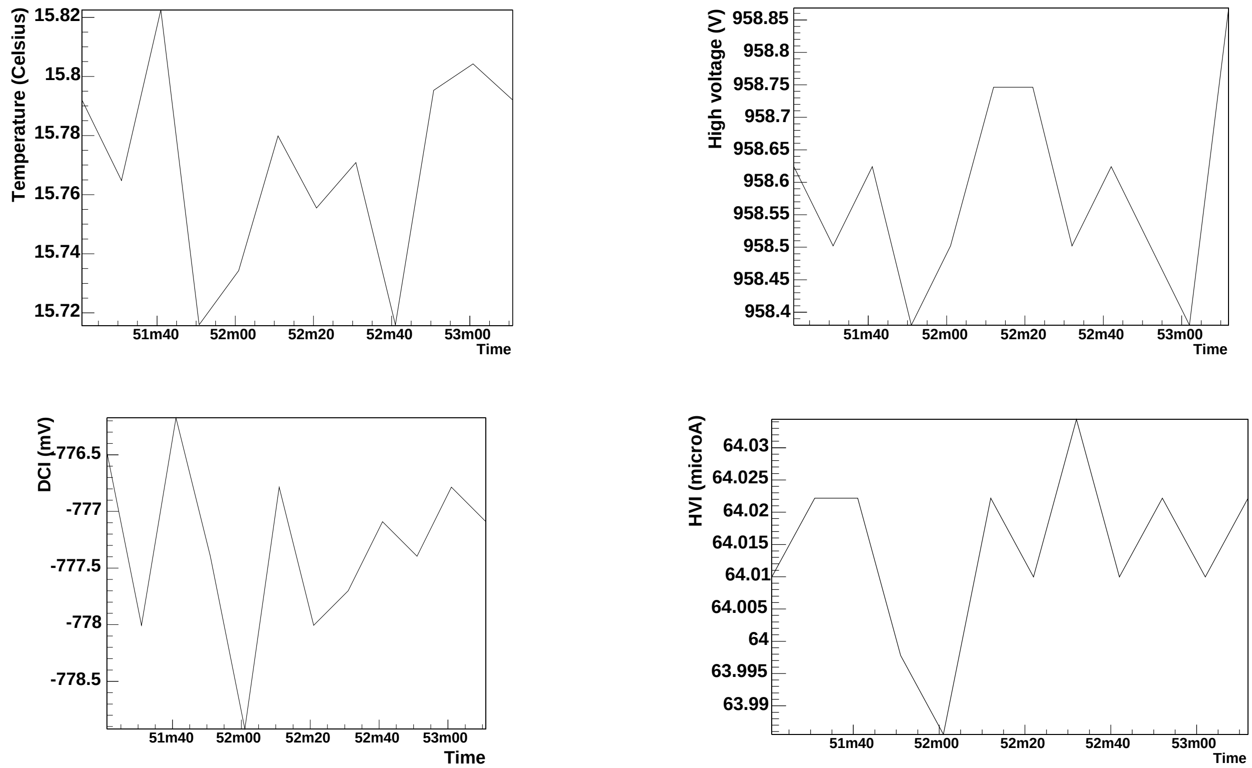

Figure 11: Monitored temperature, high voltage, DCI and HVI during an ElectronicPedestalRun for some pixels. Note the vertical scales are very small.

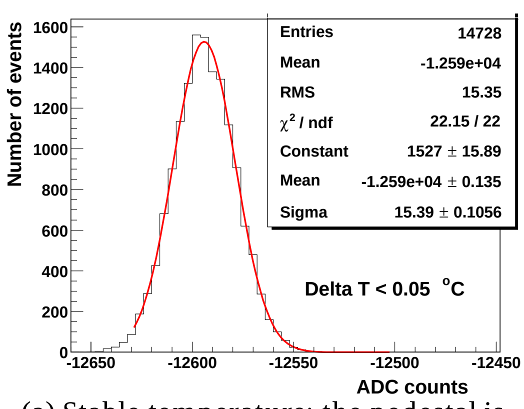

(a) Stable temperature: the pedestal is Gaussian.

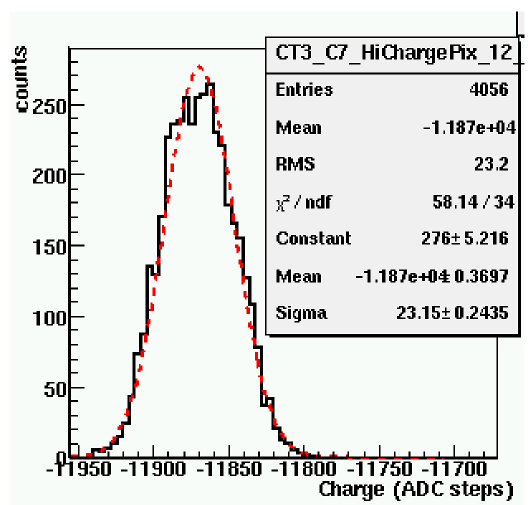

(b) Unstable temperature: the pedestal is not perfectly Gaussian.

Figure 12: high-gain charge histograms for one pixel during an ElectronicPedestalRun: the dashed line is the Gaussian fit to the pedestal.

3.2.2 Method

Principle For each ElectronicPedestalRun, the mean pedestal position and the mean dark current measurements (HVI and DCI) are computed for each pixel. The mean temperature is also measured. Then, after a scan over the runs, the evolutions of the parameters with temperature are fitted for each pixel and saved into the CALIBRATION database.

Description of the method The monitoring data can be represented by their evolution with time. Figure 11 shows the evolution of the temperature, the HV, the DCI and the HVI currents. After checking that these parameters are stable during the run (maximum temperature RMS below $0.1\,^{\circ}$C, RMS of the HV less than 4 V), we can estimate their mean values for each pixel.

For each pixel, the ADC counts read at each event are used to fill the two electronic pedestal histograms: low-gain and high-gain pedestal histograms. The histograms are fitted by Gaussians: the means are the electronic pedestal positions and the widths represent the electronic noise of the channels. The widths of the electronic pedestals are of the order of 16 ADC counts in the high-gain channels (see figure 12 a) and of the order of 6 ADC counts in the low-gain channels (see figure 13 a).

3.2.3 Run selection

Some ElectronicPedestalRuns cannot be used for a precise calibration. The selection of the runs is now described.

The number of events has to be sufficient to perform a good pedestal fit: the runs with less than 2000 events are not used in the calibration. The pedestal position, the DCI and the HVI currents vary with the temperature (see section 4.2): we require the temperature to be very stable during the run. The maximum temperature RMS among the drawers of the camera is limited to be below $0.1\,^{\circ}\mathrm{C}$. We also check that the median values of the pedestal positions and of the widths are compatible with an electronic pedestal run (pedestal position between -15000 and -9500 and width inferior to 20 ADC counts) before saving the information in the database for the run.

This selection selects about 60% of the ElectronicPedestalRuns from July 2002 to July 2003. This proves the importance of the WarmUpRuns: the temperature of the camera has to be very stable during the calibration runs. For example, the pedestal is widened if the temperature is not stable because its position moves during the run: figure 12 gives a comparison between the charge histogram obtained with a stable temperature (RMS$<0.05\,^{\circ}$C), and one obtained with an unstable temperature (RMS$>0.4\,^{\circ}$C).

3.2.4 Method to find the unlocked ARS

The unlocked ARSs in the high-gain channels are never found in the ElectronicPedestalRuns. The method described now finds unlocked ARS in the low-gain channels only.

The correct low-gain electronic pedestal charge histograms are Gaussian distributions whose width is of the order of 6 ADC counts (see figure 13 a). The pixels read in an unlocked ARS in the low-gain channel have a larger pedestal histogram. If at least 2 channels read by the same low-gain ARS have such a large distribution the low-gain ARS is flagged as unlocked. Figure 13 b shows such a charge histogram.

In a correct Gaussian histogram, the RMS of the histogram and the sigma σ_P of the Gaussian fit are very close. When a pixel is in an unlocked ARS, the width of the charge histogram is increased: the RMS is larger than the sigma of the fit. A parameter has been defined to detect these pixels:

$$\frac{\sigma_P - RMS}{\sigma_P}$$

The pixel has a problem if this parameter is less than -0.1 or if the RMS of the histogram is higher than 18 in high-gain channels. Such pixels are flagged with MiscLG or MiscHG.

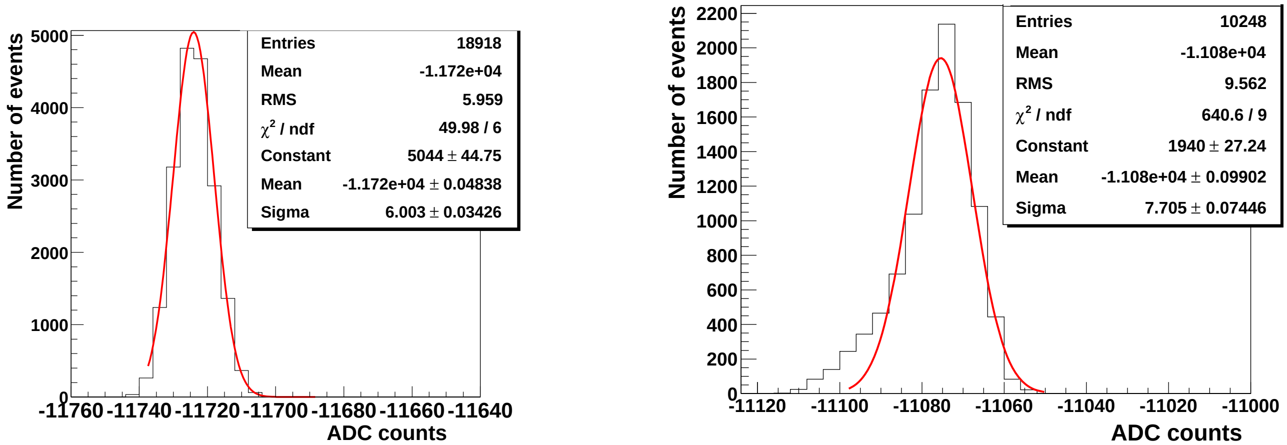

(a) Correct pixel.

(b) Unlocked ARS in low gain.

Figure 13: low-gain electronic pedestal histograms for 2 pixels.

The number of such pixels is counted for each ARS (4 pixels): if they are 2 or more in one ARS, the ARS is flagged as unlocked. Remember that this method finds unlocked ARSs in the low-gain channels only.

3.2.5 Information saved for each run

For each run, some information is stored for each drawer:

- the mean temperatures of the run: for each of the three monitored temperatures, the mean values over the run are saved.

For each run, some information is stored for each pixel:

- the electronic pedestal positions for the low-gain and the high-gain channels. The errors from the Gaussian fits are also saved.
- the pedestal widths (electronic noise) for the low-gain and the high-gain channels and fit errors are also saved.
- two flags describing why the pixel is non-operational in each channel.
- the mean HVI and DCI values over the run.

3.2.6 Information saved for a period

Once the *per run* pedestal table is filled, the data are merged and saved into the *per period* pedestal table. During this merge, the pedestal positions (for the low-gain and the high-gain channels), the DCI and the HVI are drawned as functions of the temperature for each pixel. The correlations are linear as in figures 22, 23, 25 and 26. The results of the fits (slopes and intercept points) are saved into the *per period* pedestal table. When the fit cannot be performed (less than 2 points in the plot), a flag describes the pixel without data for the period.

This table is used to know the base-lines of the pedestal positions, the DCI and the HVI in the dark: during the analysis of the data runs, the base-lines of these parameters can then be estimated when the temperature is monitored. It is used especially to estimate the NSB per pixel: the NSB is correlated to the shifts of these parameters from their positions in the dark.

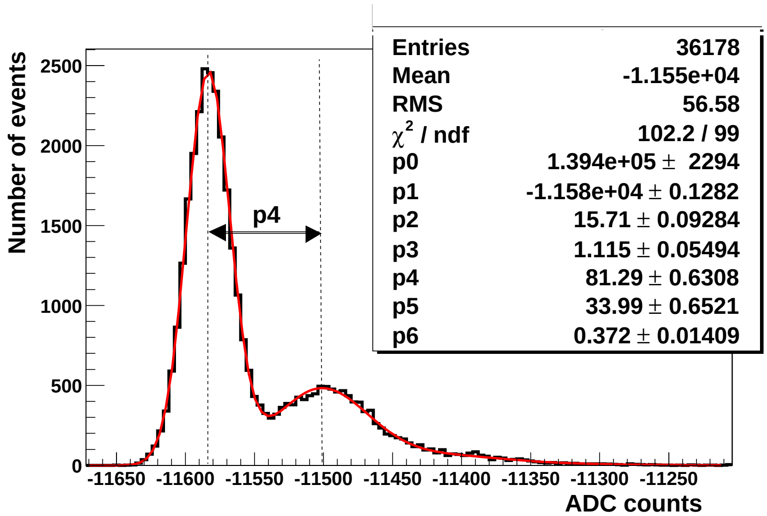

Figure 14: SinglePhotoElectronRun high-gain charge histogram: the two peaks correspond to 0 and 1 photo-electron. The distance between both gives the high-gain value for the pixel (of the order of 80 ADC counts): this value is measured by the fifth parameter (p4 or G) of the fit (function 1). (the parameters of the fit are: p0=N ; p1=P ; p2=σ_P ; p3=N_s ; p4= G ; p5=σ_G ; p6=μ)

3.3 high gain

We want here to calibrate the gain of the high-gain channel for each pixel of the cameras. This is done with specific runs. For a pixel, the gain for the period is given by the mean of the gain measured in each run.
The high gain is used in the analysis to compute the number of photo-electrons received by the pixel in the range 1 to 200 photo-electrons.

3.3.1 Type of run

The SinglePhotoElectronRuns are performed with the whole camera illuminated by one LED. The charge received by all the pixels should be set to be of the order of 1 photo-electron. As the charge is very low, the trigger has to be an external trigger. The delay between the LED pulse and the trigger signal is tuned to get the signal in the readout window. Only the high gains are calibrated with these runs and they are saved into the CALIBRATION database. The low gains are calibrated later.

3.3.2 Method

Principle For each SinglePhotoElectronRun, the gain of each pixel is computed from the shape of the high-gain charge histogram. Then, for each pixel, the mean gain on the period duration is evaluated and saved into the CALIBRATION database.

Method description The pulses with a very low intensity emitted by the LEDs follow a Poissonian distribution: the charge measured is a Poissonian law convolved with the acquisition system comportement.

The high-gain charge histograms measured during these runs have two peaks as shown in figure 14: the first peak is the pedestal position (zero photo-electron) and the second one, broader, is the peak of one photo-electron. The peak of 2 photo-electrons is generally hidden in the tail of the distribution. These distributions are fitted by function 1:

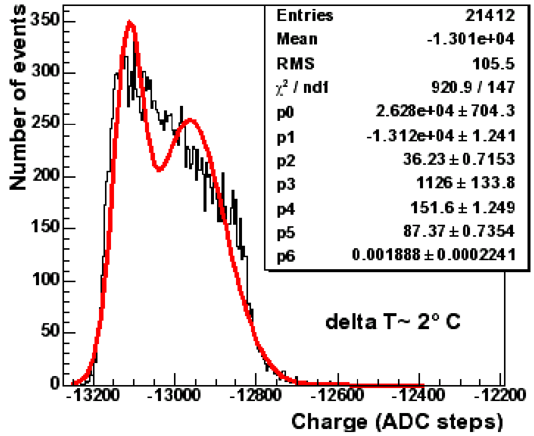

Figure 15: SinglePhotoElectronRun high-gain charge histogram with a high temperature variation. The fit is the function 1.

$$\mathcal{G}(\mathrm{x}) = \mathrm{N} \times \left(\frac{e^{-\mu}}{\sqrt{2\pi}\,\sigma_\mathrm{P}} \exp\left[-\frac{1}{2}\left(\frac{\mathrm{x}-\mathrm{P}}{\sigma_\mathrm{P}}\right)^2 \right] + \mathrm{N_s} \times \sum_{\mathrm{n}=1}^{\mathrm{m}\gg 1} \frac{e^{-\mu}}{\sqrt{2\mathrm{n}\pi}\,\sigma_\mathrm{G}} \frac{\mu^\mathrm{n}}{\mathrm{n}!} \exp\left[-\frac{1}{2}\left(\frac{\mathrm{x}-(\mathrm{P}+\mathrm{nG})}{\sqrt{\mathrm{n}}\,\sigma_\mathrm{G}}\right)^2 \right] \right) \tag{1}$$

The charge histogram is described by the zero photo-electron peak position *P*, the electronic noise σ_P, the acquisition channel gain G and the dispersion of the gain between the events σ_G. The average of the Poissonian distribution μ is the PM illumination in photo-electrons. N and $\mathrm{N_s}$ are the two normalisation factors. $\mathrm{N_s}$ is close to 1 when the distribution is Poissonian. The high gain G corresponds to the distance between the two peaks of the single photo-electron ADC count distribution.

3.3.3 Run selection

The SinglePhotoElectronRuns are selected before the calibration. The selection parameters are described now.
To have precise fit results, the number of events has to be superior to 10000. As the positions of the peaks depend on the temperature, the temperature has to be stable. The run is selected if the maximum temperature variation in the drawers is less than 0.2 degrees. The median values of the mean and RMS of the charge histograms must be compatible with the SinglePhotoElectronRun: mean between -15000 and -9000 ADC counts, and RMS between 50 and 150 ADC counts.

3.3.4 Method to find the unlocked ARS

For the high-gain calibration, only the unlocked ARS in the high-gain channels are verified. The features looked for are abnormal high-gain charge histograms in at least 2 pixels read by the same ARS.

The correct charge histograms are fitted by a Poissonian fit (function 1): the normalisation parameter N_s is close to 1. When the ARS is unlocked, the histogram is not a good Poissonian: the pixel is flagged as 'bad' if N_s is less than 0.5. If 2 or more pixels have this feature in the same ARS, the ARS is flagged as unlocked.

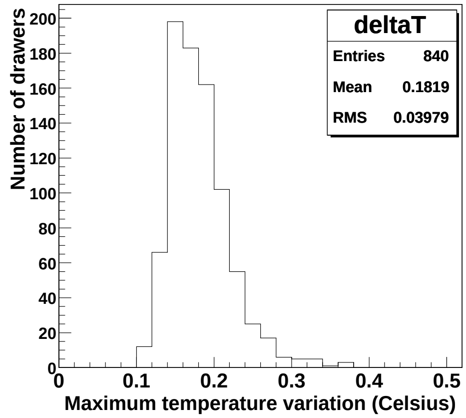

Figure 16: Distribution of the temperature variations measured every two minutes in the camera drawers for one run.

3.3.5 Information saved for each run

The information saved for each pixel is:

- the high voltage value,
- the high gain G, its dispersion σ_G and the errors of the fit on these parameters,
- a flag describing the non-operational pixel status (HV off or unstable, unlocked ARS in high-gain channel). For CT3, the SinglePhotoElectronRuns are taken in normal trigger: it is thus necessary to have one drawer much more illuminated than the others (about 60 photo-electrons). The flag describes also the pixels of this drawer.

3.3.6 Information saved for a period

Once the *per run* gain table is filled, the data are merged and saved into the *per period* gain table. During this merge, the gains are plotted as a function of the run number. The gains should be stable over a period as shown in figure 27. The mean high gain and its dispersion are calculated, fitting the graphs by constants. The mean values and their errors are saved into the database. A flag describes the pixels without any gain data for the period: they are not used in the analysis.

3.4 Run pedestal

The aim of this calibration is to determine the pedestal positions in high and low-gain channels for each pixel of the cameras.

3.4.1 Type of run

The run pedestal is calculated for the ObservationRuns. They are runs performed in charge mode, with an internal trigger.
They are normal runs tracking at the sources: each pixel has NSB and Cerenkov events.

The run pedestal is saved into a ROOT file for each run.

3.4.2 Method and information saved for each observation run

Principle We have seen (see section 2.4) that the charge histograms have two components: the run pedestal (the charge histogram taking into account the NSB) and some Cerenkov events with higher charges. The desired parameter is the mean value of the run pedestal distribution.

The pedestal position of a pixel is the mean value of the charge histogram filled without the Cerenkov events. As the pedestal varies with the temperature, it is evaluated every two minutes and saved into a ROOT file. Each pixel has two pedestal values: one for the low-gain channel and one for the high-gain channel.

Method description The aim of the method is to fill the charge histograms of the PMTs while excluding the PMTs with Cerenkov events, i.e. with the ADC counts higher than the ADC counts due to the NSB events. For each pixel of the camera, at each event, if none of its neighbours has a charge above a threshold (2 photo-electrons), the event is considered to be a NSB event and the pedestal histogram is filled. The charge received by each pixel thus has to be estimated every event. To evaluate the charge, a first evaluation of the pedestal position is needed.
Three charge histograms are thus filled per pixel: two are the pedestal charge histograms for high and low-gain channels, one is used to estimate the charge of the pixel. The method used to fill them is now described.

1- First approximation of the pixel charge For each pixel, the charge histogram used to estimate the pedestal position is filled with the raw high-gain ADC counts. It is filled with the events whose ADC count is between -15000 and -10000 so that the high-charge Cerenkov events are cleared. Every 400 events, the mean of this histogram is evaluated and the histogram is cleared. The mean gives the first appoximation of the pedestal position of each pixel. This value is then used to evaluate the charge received by the pixel before filling the two pedestal histograms.

2- Filling of the pedestal histograms At each event, the pedestal charge histograms for high and low-gain channels are filled only if the pixel and all its neighbours have an estimated charge lower than 2 photo-electrons: all the Cerenkov events are cut.
As the temperature can vary during the 28-minute data runs, the run pedestal positions are estimated every two minutes. Figure 16 gives the distribution of the temperature variations in two minutes: the mean is less than $0.2\,°\mathrm{C}$. The maximum does not exceed $1\,°\mathrm{C}$. The means and the widths (RMS) of the run pedestal charge histograms are thus calculated and saved into a ROOT file every 2 minutes. Then the pedestal histograms are cleared, and filled again during the next 2 minutes of run.

In single telescope runs, for a trigger condition of 5 pixels above 3.5 photo-electrons, about $70\,\%$ of the events are used to fill the run pedestal histograms, the others are considered to be Cerenkov events. This value depends on the trigger conditions.

When analysing an event, the pedestal position is the value we have to subtract from the ADC count to compute the number of photo-electrons (charge) received by the pixel. It is very important to estimate it precisely. During the analysis, the run pedestal positions are read every two minutes: these values are used to calculate the charges of the Cerenkov events in the pixels.

3.5 Non-operational pixels

We want to detect and flag in each run the pixels that are not usable in the analysis. The causes have already been described (section 2.7). Here we explain in more detail the methods used to detect the unlocked ARSs.

3.5.1 Type of run

The non-operational pixels are stored into ROOT files for the ObservationRuns and the FlatField-Runs.
The ObservationRuns are described in the section 3.4.1.
The FlatFieldRuns are performed in charge mode, with an internal trigger. During the runs, the camera is illuminated with a laser or a LED with a very homogeneous light between 50 and 200 photo-electrons. Moreover, after September 2003, 1 events out of 5 are soft (random) trigger events.

3.5.2 Methods to find the unlocked ARS

Principle The method used to find the unlocked ARS in FlatFieldRuns and ObservationRuns is performed in 5 steps.

- 1- rejection of the pixels which have problems other than unlocked ARS
- 2- selection of the pixels that could be in an unlocked ARS
- 3- for the pixels that could be in an unlocked ARS, we have to determine on which channel (high-gain or low-gain) the ARS could be unlocked
- 4- finally, in each group of 4 pixels (see figure 9), if 2 or more pixels could be read in an unlocked ARS in the high (low)-gain channel, the ARS of the high (low)-gain channel is flagged as unlocked.

The steps of this analysis are now described more precisely. Note that in the third step, the methods are different for ObservationRuns and FlatFieldRuns. Both methods are described below.

Some characteristic features of the unlocked ARS pixels When the ARS is unlocked, some events have a good ADC counts but others do not. This results in increasing the width of the histograms of the logarithm of the high-gain to low-gain ratio. An example is given figure 17.

1- Rejection of the pixels which have other problems than unlocked ARS Some pixels have problems that are not linked with unlocked ARS. They can have a pedestal charge histogram (no gain) instead of a run pedestal histogram or too narrow a charge histogram (in comparison with the mean value of the RMS of the charge histograms). In both case, the RMS of the charge histogram is lower than usual. This characteristic is used to detect these pixels.
Once all the charge histograms are filled, the mean of the RMS of all the histograms are computed for both low-gain and high-gain channels. The parameter used to select the pixels with problems other than unlocked ARS is the ratio:

$$\mathrm{R} = \frac{\mathrm{RMS\ of\ the\ charge\ histogram\ of\ the\ pixel}}{\mathrm{mean\ of\ the\ RMS\ of\ the\ charge\ histograms}}$$

If all the pixels are illuminated equally and have the same characteristics, the RMS are roughly the same for all the pixels: the ratio R is thus close to 1 for all the pixels.
The pixels whose charge histogram is too narrow are rejected: the pixels whose ratio R is less than 0.55 are flagged as non-operational. The flags used for these pixels are 'NoSig' (pedestal) or 'BadGain'.

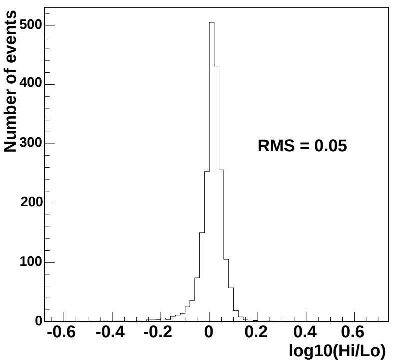

(a) Correct pixel.

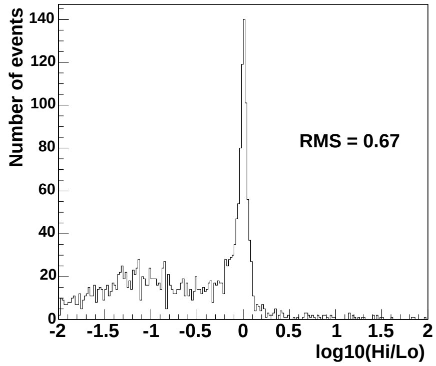

(b) high-gain unlocked ARS.

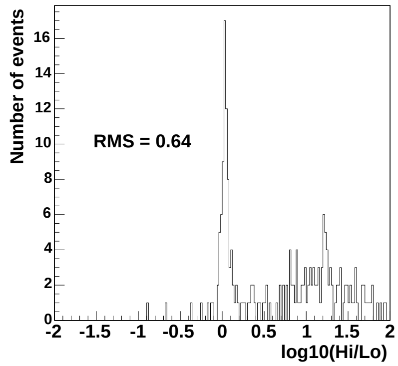

(c) low-gain unlocked ARS.

Figure 17: Histograms of the logarithm of the ratio high-gain to low-gain charge for three pixels.

2- Selection of the pixels that could be in an unlocked ARS We have then to determine if the pixel whose ratio R is more than 0.55 are in an unlocked ARS. Another parameter is calculated, which checks wether the high-gain over the low-gain ratio is correct. When the event has a charge between 15 and 200 photo-electrons, a histogram is filled with the logarithm of the ratio of the high-gain channel charge over the low-gain channel charge. In this range, both channels can be used. The charges measured in the high-gain channel and in the low-gain channel should be roughly the same: the histograms of the correct pixels have all the events close to 0 (see figure 17 (a)). When one of the ARS of the pixel is unlocked, the histogram is broader: the parameter used to select such pixels is the RMS of the histogram H. If the RMS is higher than 0.2, the pixel is counted as a candidate to be in an unlocked ARS.

3a- Search for the channel of the unlocked ARS in ObservationRuns To determine on which channel is the unlocked ARS, we use the preceding histogram of the high-gain to low-gain ratio.
When the ARS in the high-gain channel is unlocked, the high-gain ADC count is generally less than the normal ADC count: the high-gain charge is thus less than the low-gain charge for these events. The histogram then has a tail with negative values as shown figure 17. When the unlocked ARS is in the low-gain channel, the tail is towards the positive values. These features are used here to determine which ARS can be unlocked.

Three areas are calculated. They are defined on figure 18:

- the integral of the entire histogram (i)
- the integral of a part of the right part of the histogram (r)
- the integral of a part of the left part of the histogram (l)

The pixel is counted as unlocked in the high-gain channel if ($l > 0.2 \times i$) and in the low-gain channel if ($r > 0.2 \times i$). It is possible that both channels are counted as unlocked.

Then, in each group of 4 pixels, if 2 or more pixels are candidates to be in an unlocked ARS in the high (low)-gain channel, the ARS of the high (low)-gain channel is flagged as unlocked. If only one pixel of the ARS has a problem, it is flagged **MiscLG** or **MiscHG**.
The flag **BadHiLo** is given when a pixel is detected in the second step but not in the third one (i.e. if the histogram has a strange mean (less than -0.1 or more than 0.1) or is too large but the tails on the left and on the right do not contain more than 20% of the events).

3b- Search for the channel of the unlocked ARSs in FlatFieldRuns For the pixels that could be in an unlocked ARS, we have to determine which ARS could be unlocked: high-gain or low-gain ARS.

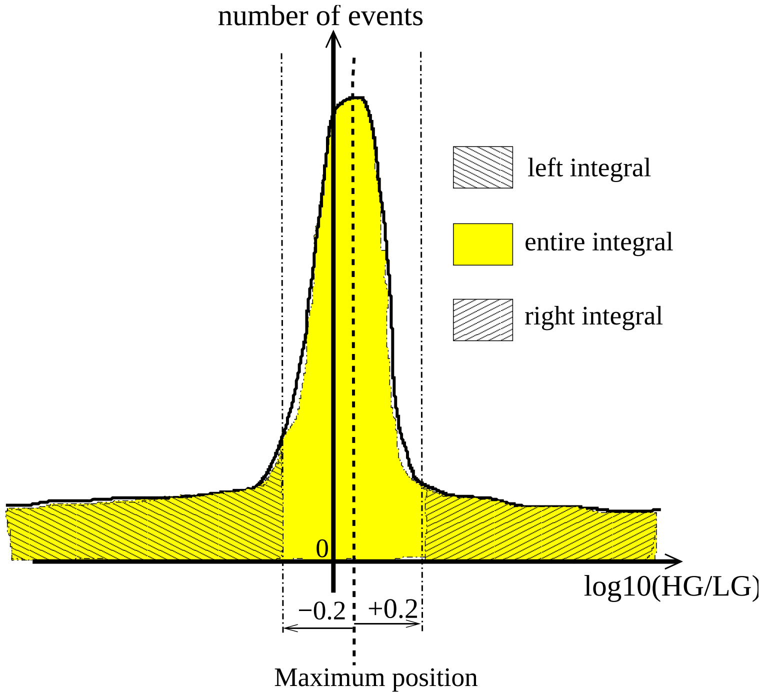

Figure 18: Definition of the integrals used to find which channel (high-gain or low-gain) has an unlocked ARS for the ObservationRuns. This scheme is a non-scaled representation of the real histograms (see figure 17).

The ARS of both channels are checked for each selected pixel with the same method described below. To check if the high-gain channel ARS can be unlocked, we use the high-gain charge histogram: if the histogram is broader than usual, the ARS in the high-gain channel can be unlocked. The same test is done with the low-gain channel.

If the ratio R of the pixel is larger than 1.5, the pixel is counted as unlocked in the corresponding channel. Usually, this test is sufficient, but some unlocked ARSs are sometimes not detected. Another check is then done if R is less than 1.5. The RMS of the entire charge histogram is calculated. Then a window of interest is selected around the maximum ADC count and the histogram is fitted by a Gaussian in this window. If the charge histogram is correct, all the events are in the window and the sigma σ of the fit is close to the RMS of the histogram. If not, the sigma of the fit is much less than the RMS. The pixel is counted as unlocked in the corresponding channel if: $\frac{\sigma}{RMS} < 0.05$.

Then, in each group of 4 pixels, if 2 or more pixels are candidates to be read by an unlocked ARS in the high (low)-gain channel, the ARS of the high (low)-gain channel is flagged as unlocked.

3.5.3 Information saved for each run

Each pixel has a flag summarizing the sources of its dysfonctional status (the names of the flags given here are those from the class Calibration::PixelBroken from the HESS software):

- disabled HV (flag HVOff)
- unstable HV (flag HVUnstable)
- unlocked ARS (flag ARSLG or ARSHG)
- problems found in the first part of the search for unlocked ARS: pedestal (flag NoSig) or gain problem (flag BadGainLG or BadGainHG)
- problems in the high-gain to low-gain ratio in a single pixel (flag MiscLG, MiscHG or BadHiLo)

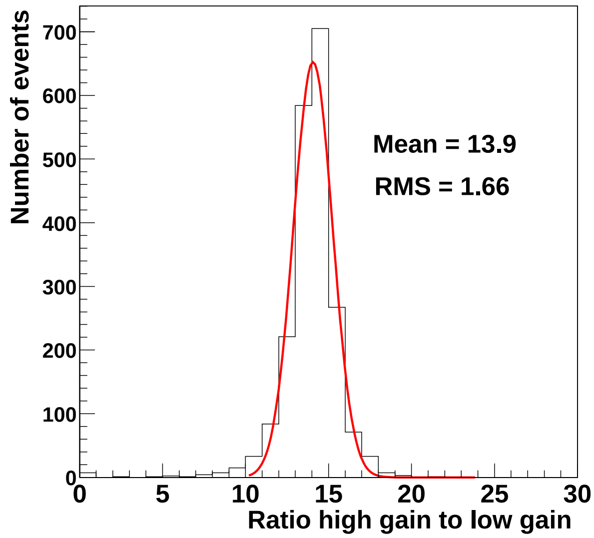

Figure 19: Histogram of the high-gain to low-gain ratio for a pixel.

The flags are stored into a class (Calibration::TelescopeBrokenPixel) saved into a ROOT file. This file is read when the run is analysed: the non-operational pixels are not used.

3.6 Low gain: high-gain to low-gain ratio

The aim of this calibration is to know the gain of the low-gain channel for each pixel of the cameras. The low gain is used in the analysis to compute the number of photo-electrons received by the pixel in the range 15 to 1600 photo-electrons.

3.6.1 Type of run

The low-gain calibration is done using the ObservationRuns (see section 3.4.1). The information of the low-gain calibration is saved into the CALIBRATION database.

3.6.2 Method

Principle As the high gain is already calibrated with the SinglePhotoElectrons runs (see section 3.3), the low gains are known indirectely: it is the the high-gain to the low-gain ratio that is calibrated.

Method description During the data runs, many events are in the range 15 to 200 photo-electrons. To select these events, the number of photo-electrons is calculated in the high-gain channel with a known gain. For the selected events, the ADC counts in the low and high-gain channels are measured (C_L and C_H), and the run pedestal positions (P_L and P_H) are read from the run pedestal ROOT files. The run pedestal files have to be created before the low-gain calibration is launched.
The high-low ratio is:

$$\frac{C_H - P_H}{C_L - P_L}$$

For each pixel a histogram such as that in figure 19 is filled with these ratios. The histograms are then fitted by Gaussians whose means give the high-gain to low-gain ratios of the pixels.

3.6.3 Information saved for each run

For each run, some information is stored for each pixel:

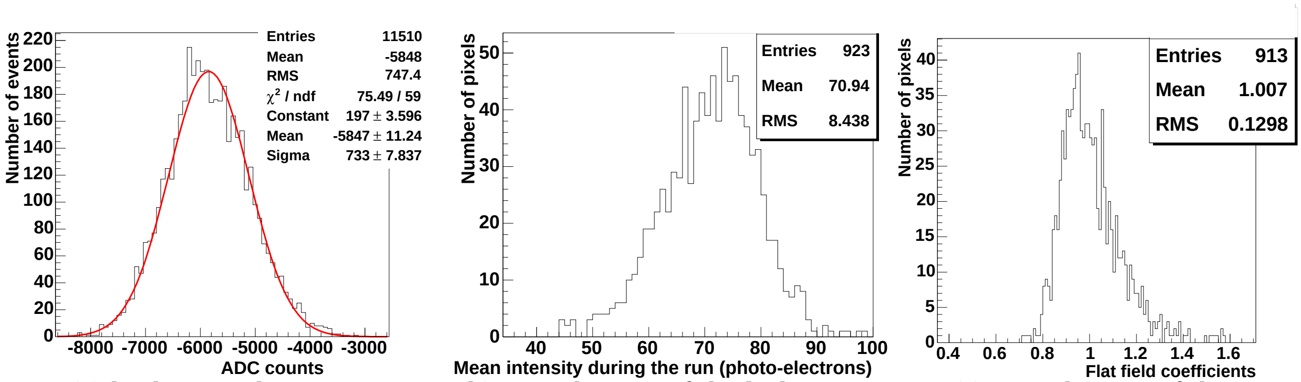

(a) high-gain charge histogram for one pixel.

(b) Distribution of the light in the camera.

(c) Distribution of the flat-field coefficients.

Figure 20: Some steps of the flat-field coefficient calibration (run 10912, CT2).

- the high-gain to low-gain ratio
- the width of the Gaussian fit as error on the value
- a flag describing why the pixel is non-operational

3.6.4 Information saved per period

Once the per-run table is filled, the data are merged and saved into the per-period table. The high-gain to low-gain ratios are plotted for each pixel as a function of the run number. The ratios are stable over a period, as shown in figure 29. The mean ratios are calculated fitting the histograms of each pixel by constants. The mean values and their errors are saved into the database. A flag describes the pixels lacking data over the period.

During the analysis, the high-gain to low-gain ratios are used to calculate the number of photo-electrons received by the pixels in the low-gain channels data.

3.7 Flat field

We want to compute the flat-field coefficients to take into account in the analysis the inhomogeneities in the light collection efficiency between the pixels. This is done using specific runs with homogeneous light on the camera.

3.7.1 Type of run

The flat-field calibration is done using the FlatFieldRuns: they are taken in charge mode, with internal trigger. The camera is illuminated by a very homogeneous pulsed light produced by a LED or a laser at the center of the dish. The charge is generally between 50 and 200 photo-electrons in each pixel. In order to limit the number of inhomogeneous Cerenkov events, the telescope should point at the sky near the horizon. In order to limit the number of switched-off pixels, the region should not have many stars.
After September 2003, 1 events out of 5 are soft (random) trigger events.
The flat-field coefficients are saved into the CALIBRATION database.

3.7.2 Method

Principle The mean number of photo-electrons I received by each pixel on the run duration is calculated. Then the mean charge $< I >$ received per pixel during the run is found. The flat-field coefficient of a pixel is the ratio:

$$\frac{<I>}{I}$$

Only one coefficient is defined per pixel. The charges have to be calculated using either the high-gain channel or the low-gain channel. The channel used depends on the Laser (LED) intensity (the high-gain channel is used when the charge is above 150 photo-electrons).

Method description The flat-field computation is done on the homogeneous events from the mirror LED or laser. Nevertheless, some Cerenkov events due to cosmic rays can trigger the camera: these events have to be rejected.
The pedestal position is computed for each pixel from the monitored temperature and the gains are already calibrated. At each event, the charge received by the pixels can thus be determined and filled in an histogram. The event is considered as usable for flat fielding if:

- the ratio of the RMS to the mean of the light distribution is less than 0.3 (it is more than 1000 for cosmic events)
- the mean light distribution is more than 10 photo-electrons

These events are used to fill the charge histograms. The other events are not used. For the selected events, the mean charge is filled in an intensity histogram.

Then we have to determine which channel will be used to calculate the flat-field coefficients. If the mean of the histogram is between 10 and 150 photo-electrons, the high-gain channel is used; if it is between 150 and 1600, the low-gain channel is used. The charge histograms of the selected channel are then fitted by a Gaussian to get the mean ADC count S of the pixels on the run duration (see figure 20(a)). The pedestal positionP and the gain G of the channel are known. The mean charge received by each pixel during the run is then computed (their distribution is given figure 20(b)):

$$I = \frac{S - P}{G}$$

The mean charge received by the camera is then $<I>$, and the flat-field coefficients ($I/<I>$) are calculated (see figure 20(c)): the mean of the distribution is 1 by definition.

Before the estimation of the charge I of the pixels, the pedestal position P can be estimated by two means:

- if soft events are taken during the run, a pedestal charge histogram is filled for each pixel with these events: the means of the distributions give the pedestal positions of the pixels. Soft events have been taken automatically in the FlatField Runs after 30th September 2003 (run 15973).
- else, the pedestal position is calculated from the temperature and its correlation stored in the database.

3.7.3 Run selection

Currently, all the flat-fielding runs are used to compute the calibration. We will soon select the runs with more than 5000 events, with temperature variations inferior to $0.2\,^{\circ}\mathrm{C}$ and with mirror LED or laser light intensity between 10 and 1600 photo-electrons.

3.7.4 Information saved for each run

The information saved for each run and for each pixel is:

- the flat-field coefficient and its error
- a flag describing why the pixel is non-operational

3.7.5 Information saved for a period

Once the per run table is filled, the data are merged and saved into the per period table. The flat-field coefficients are drawned as functions of the run number. The coefficients are stable over a period as shown figure 31. The mean coefficients are calculated fitting the distributions by constants. Their values and the errors of the fits are saved into the database. A flag describes the pixels without any data over the period.

During the analysis, the flat-field coefficients are used as a correction in the calculation of the number of photo-electrons received by each pixel. The inhomogeneities of the camera are then decreased.

3.8 Use of the calibration coefficients during the analysis

During the analysis of a run, the non-operational pixels and pedestal ROOT files are read. The high gains, the ratios high-gain to low-gain and the flat-field coefficients are read from the CALIBRATION database.
All the calibration parameters for each pixel are then known:

- the pedestal positions in high and low-gain channels, P_{High} and P_{Low}.
- the high gain G
- the ratio of high-gain to low-gain R
- the flat-field coefficient F
- a flag for the non-operational pixels

At each event, the ADC counts are measured in both channels: C_{High} and C_{Low}. The calculation of the charge in photo-electrons received by every operational pixel is then:

$$I_H = \frac{C_{\mathrm{High}} - P_{\mathrm{High}}}{G} \times F$$

$$I_L = \frac{C_{\mathrm{Low}} - P_{\mathrm{Low}}}{\frac{G}{R}} \times F$$

Either the high or the low-gain channel is used depending on the charge value. The non-operational pixels are not used in the analysis.
The electronic pedestal database is used when the NSB needs to be estimated.

4 Calibration results

The calibration has now been done over one year of data. Some results can be described. First the correlations of the base-lines in the dark with the temperature are shown. Then the evolutions of the gains and the flat-field coefficients are analysed. Some issues about the non-operational pixels are discussed. We show the tools to detect the broken pixels exist: some pixels have to be replaced in December 2003. Finally, we show the quality of the calibration runs can be improved.

All the figures referenced in this section are at the end of the note.

4.1 Correlation of the temperatures

The three temperatures in each drawer are very well correlated: the plot of one versus another is a line of slope close to 1 (see figure 21). The same characteristics are seen in the plots of the temperatures from different drawers of a camera: the temperatures in the entire camera are also very well correlated.

For the calibration of the pedestal, because of this correlation, only one temperature per drawer need to be used: we have chosen to use the temperature T2, measured near the ARS.

4.2 Evolution of the dark base lines with the temperature

The electronic pedestal position, the DCI and the HVI vary with the temperature. Some plots are given in figures 22, 23, 25 and 26. They have been performed using the Electronic Pedestal Runs from March, 12 to August, 31 2003, for CT3.

4.2.1 Electronic pedestal position

When the temperature varies, the variations of the electronic offsets of the amplifiers in the acquisition channels cause offsets of the pedestal positions.

The pedestal positions have a linear correlation with the temperature. This correlation is stable as long as the camera configuration stays the same. The distributions of the slopes of the correlations for the low-gain and high-gain channels are given in figure 24. Nevertheless, the dispersion of the pedestal position around the fitted line is not always negligible. The high-gain pedestal position is generally good to ± 100 ADC counts from the mean line, which represents ± 1.5 photo-electrons. As the high-gain channel is used in the range 1 to 100 photo-electrons, the estimation of the electronic pedestal position from the temperature can be used as a first approximation (see section 3.7), but the precision on the charge decreases when the signal is lower. The same happens in the low-gain channels: the pedestal position is known from the temperature to ± 15 photo-electrons and it is used in the range 15 to 1600 photo-electrons.

Because of this lack of precision, the electronic pedestal position computed with the temperature monitoring is not used anymore during the analysis. We now always read the pedestal positions from the ROOT pedestal files.

The pedestal from the database can still be used to estimate the NSB in each pixel, but much better methods exist using DCI or HVI shifts.

4.2.2 DCI

The DCI currents have a linear correlation with the temperature. The distribution of the slopes of the lines is given in figure 25: the slopes are distributed between -10 and $30\,\mathrm{mV}/^\circ\mathrm{C}$.
We did not find any correlation between the slopes and the drawer position or the neighbours.

4.2.3 HVI

The HVI currents can be considered as independant from the temperature. The slopes are mainly distributed between $-0.02\,\mu\mathrm{A}$ and $0.03\,\mu\mathrm{A}/^\circ\mathrm{C}$ (see figure 26), up to $0.08\,\mu\mathrm{A}/^\circ\mathrm{C}$ for some pixels, whereas the shift due the mean NSB measured in Namibia (10^8 Hz) is of the order of $3.2\,\mu\mathrm{A}$: the variations with the temperature can be neglected. This property makes the HVI a very good parameter to estimate the NSB in the data.

4.2.4 The other parameters

The high gains, the high-gain to low-gain ratios and the flat-field coefficients are independant of the temperature. Their evolution with time is described in the next section.

4.3 Stability of the gains and flat-field coefficients

4.3.1 The gains

Figure 27 shows the evolution of the high gain of a pixel over a calibration period. The variations around the mean value are generally less than 4%. The gain of many pixels decreases slowly with time (see figure 28): of the order of -3 ADC counts per shift period. This is due to the aging of the PMTs. The decrease is getting slower with time. This means the HV have to be regularly increased to correct the gains, at least during the first year of working. Moreover, it highlights the importance of taking SinglePhotoElectronRuns very regularly. Shift crews are asked to performe calibrations every 1 or 2 days at least (see [5]).

The low gain is calibrated through the high-gain to low-gain ratio. Figure 29 shows the stability of the ratio over a period: the variations around the mean value are less than 3%. The ratio is generally stable over some months: the evolutions of 2 pixels in figures 30 (a) and (b) are stable within 2%. But some pixels have evolution with steps such as 30 (c): the step happens in the middle of a shift period: we do not observe any correlations with the beginning or the end of a period. For such pixels, the ratio variations are of the order of 7%.

4.3.2 The flat-field coefficients

The flat-field coefficients are stable over a calibration period as shown figure 31 (a) and on even-longer time as shown figure 31. Their variations are less than 5%. One cause of this dispersion is that the flat-field coefficients are relative calibration coefficients, whereas the non-operational are not the same from one run to another.
Nevertheless, some pixels have larger dispersion over a long period, up to 15% (see figure 31 (b)).
The fact that the flat-field coefficients are stable indicates the aging of the photo-cathodes and Winston cones, if any, is rather homogeneous on the camera.

The distribution of the coefficients (see figure 31 (b)) has a RMS of the order of 13%: this represents the relative discrepancy in the light collection efficiency between the pixels.

To check the homogeneity of the camera after the whole calibration, it is possible to use all the calibration parameters (pedestals, gains, flat-field coefficients, non-operational pixels) and to compute again the flat-field coefficients. The distribution of the new coefficients is given figure 33: the RMS is now of the order of 3%. This confirmes the flat-field coefficients describe correctly the camera inhomogeneities.

4.4 Some results on the methods to find the unlocked ARS

4.4.1 Stability of the method for ObservationRuns

The method has been described in section 3.5.
The way to lock an unlocked ARS is to switch off and on the power of the camera drawers. When the power is not cycled, the ARS should stay in the same state (locked or unlocked) for the entire shift night.
Looking at the non-operational pixels files for some nights, the method to find the unlocked ARS is stable: the ARS state is constant during the night.

4.5 The non-operational pixels and the broken pixels

The non-operational pixel distributions give some information about the cameras.
The detection of the broken pixels is important: CT3 has been operating for more than one year, and CT2 for half a year. The analysis of the evolution of the non-operational pixels is used to have information about the pixel aging and to detect the broken pixels we need to replace.

The analysis has been done on the non-operational pixels computed from July, 6th to October, 1st 2003.

What has improved about the ARSs ? For each pixel, the frequency it has been found in an unlocked ARS has been computed over 3 months. Figure 35 gives the distributions for CT2 and CT3. It highlights that the unlocked ARSs are not always the same. Nevertheless, some individual ARS are often unlocked (the maximum is in 50% of the runs) and many of them are never unlocked. Most of the ARSs are found unlocked in less than 1% of the runs.
Figure 34 shows the number of unlocked ARSs per run is of the order of 3 to 4 both in the high and low-gain channels in the cameras CT2 and CT3.

The number of consistently-locked ARSs is higher in CT2 than in CT3, as shown figure 36: a better criterion (the pedestal width of the ARS) had been used to reject the noisy ARSs on the second camera.
An upgrade of CT3 has been performed in February 2003 to limit the number of unlocked ARSs. Before the upgrade, a procedure of about 30 minutes was done at the beginning of the night to lock the ARSs. This procedure is no longer performed. Figure 34 gives the distributions of the number of unlocked ARS per run. There are of the order of 4 unlocked ARS per channel and per run in the runs performed after the upgrade. In 2002, the mean number of unlocked ARS per run in CT3 was of the same order. This proves that the upgrade was usefull: the number of unlocked ARS is equivalent to before but without the need for a long procedure to lock them.

4.5.1 What is the effect of the stars on the pixels ?

The pixel high voltage is switched off online when the HVI is too high, i.e. when the pixel sees a bright star. The number of such pixels depends, of course, on the region of the sky. At the moment, the pixels are not switched on again when the star has left the pixel.
The pixels are flagged ’UnstableHV’ when they are switched off at the beginning of the run. Remember that those which are switched off during the run are not flagged in order to be used in the analysis until they are off.

The number of pixels that are switched off due to stars is always less than 10 per run after July 2003, as shown in figure 38. Before, the average number of off-pixels per run was of the order of 30: the online switch-off of the pixels based on the HVI current has been less stringent after June, 12th 2003. Note that it also depends on the source: many galactic sources were observed before July, increasing also the number of pixels switched off.
The positions of the pixels switched off in the cameras are very similar for both telescopes, which is obvious for stereoscopic observations in the same directions.

At the moment, when the stars move in the field of view, other pixels are switched off during the run: the number of non-operational pixels increases. An upgrade will be done to compute the star trajectories in the camera and switch on the pixels after a certain time. No more than 1% of the pixels should then be switched off due to stars.

Figure 37 gives the distribution of the frequencies the pixels are flagged HVUnstable. The pixels have never been illuminated by bright stars in more than 2% of the runs in the 3 months of observation. Two pixels constently have unstable HV: G7-15 in CT3 after July 29th, and G4-05 in CT2 after September 21st. They have been replaced in December 2003.

4.5.2 What are the broken pixels ?

The distribution of the number of non-operational pixels per run is given in figure 40. On average, they are 32 in CT2 and 40 in CT3. The difference is due to the number of unlocked ARS which is higher in CT3. We have seen about 25 pixels are non-operational due to unlocked ARS or stars. What are the other causes? Is there broken pixels in the cameras?

The distributions of the non-operational pixel frequency (independentely on the causes) are given in figure 39 for CT2 and CT3. The number of pixels that are not operational in more than 30% of the runs is 25 in CT2 and 18 in CT3. It is possible to identify them by looking at figure 41. Two pixels have already been detected with unstable HV. In CT2, 3 ARSs are often unlocked: C3-00 to 03, C3-04 to 07 and G3-04 to 07. The other pixels have no signal (low gain) or a bad high-gain to low-gain ratio. These pixels have been replaced in December 2003. A quick look at the first data from CT4 shows 3 pixels may be broken: G5-07 has unstable HV, H5-08 and B7-10 have bad high-gain to low-gain ratio.

4.6 Calibration run quality

Figures 42 and 43 give the number of calibration runs taken during each shift period and the fraction that can be used for calibration. The selection of the runs has been performed using these cuts:

- charge histograms compatible with the type of run
- sufficient number of events to perform the fit (2000 for electronic pedestal runs and 8000 for single photo-electron runs)
- temperature RMS $< 0.2°\mathrm{C}$

The main selection is done with the temperature stability. This proves the WarmUpRuns are really necessary and it is not good to perform calibration runs after a power shutdown of the cameras. Note that some periods have no calibration runs. The shift crews must perform calibration runs.

4.7 Some other problems

Single photo-electron calibration system Some problems are to be noted for the SinglePhotoElectron runs on CT3 (first camera). The LED panel on the lid of the camera has problems during the configuration. This problem induces the shift screw to sometimes skip the high-gain calibration after some tries. Moreover, some LEDs are never at the good intensity, which prevents the gain calibration for the corresponding pixels.

A new single photo-electron system has been installed on the 4 telescopes in December 2003. Only 1 LED now illuminates the camera with a light of about 1 photo-electron intensity and 50% homogeneity.

Strange events Some raw data events have to be eliminated of the calibration and the analysis:

- events whose time stamp is inferior to the time stamp of the previous event (GPS failure)
- events whose time stamp is the same as the previous event, and the ADC counts are 0 in all channels
- events with less than 45 drawers with data: FIFO readout error

4.8 Status of the calibration in Paris

Currently, the calibration in Paris is done up to October 2003. The status of the calibration is avalaible on a web page (see [3]).

5 Conclusion

- The calibration tools in Paris are now stable. The camera is stable over a shift period, even if on longer time-scales the gains decrease and need regular adustements of the high voltage values. This aging of the PMTs may stop after some time. The parameters that depend on the temperature (pedestal, HVI and DCI) are calibrated as functions of the temperature: they are used to estimate the NSB. The pedestal in the data runs are estimated very often (2 minutes) to take into account the temperature variations during the 28-minute observation runs. The gains (high gain and high to low-gain ratios) and the flat-fielding coefficients are independant of the temperature. A value is given for each pixel per period: computing the mean from different calibration runs improves the precision of the parameters.
  The non-operational pixel causes are well understood. The two main causes are the unlocked ARSs and the stars that switched off the pixels at the beginning of the run. This last component can still be removed by switching on the pixel high voltage on-line when the stars have moved off the pixel. Some pixels are constantly broken: 25 in CT2, 18 in CT3 and 3 in CT4. They have been changed when the fourth camera (CT1) was installed (December 2003).

- The calibration runs are very important. The shift crews have to perform them at least every 2 nights. This instruction has not always been followed.
  Some improvements still have to be done on the quality of the calibration runs: the temperature stability has to be increased particularly. The WarmUpRuns are thus very important before any calibration run. An improvement has been made with a higher soft trigger rate for the ElectronicPedestalRuns and the FlatFieldingRuns. The LEDs of the SinglePhotoElectronRuns new calibration system pulse at about 60 Hz: the run duration has thus to be at least 5 minutes, which demands very stable temperature.
  Another improvement is now made for the FlatFieldingRuns: soft events are triggered in the run configuration. They are used to compute the pedestal positon. These events are flagged to simplify the computation of the flat-field coefficients.

- The methods and the way the parameters are stored in Paris are slightly different from those used in the Heidelberg calibration. Nevertheless, both calibrations can be read and used in the analysis: this compatibility is important to be able to cross-check the calibration.

- To check the calibration, a study of the camera using muons rings in the ObservationRuns is performed. This method will be explained in a future note.

6 Figures: calibration results

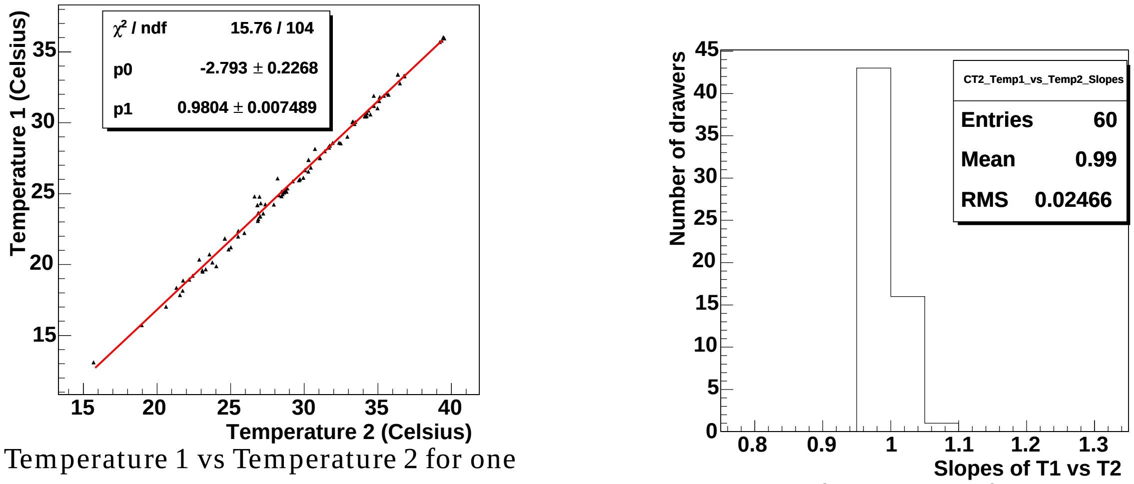

a- Temperature 1 vs Temperature 2 for one drawer.

b- Distributions of the slopes of the correlations.

Figure 21: Linear correlations of the temperatures in a drawer (data during 4 months).

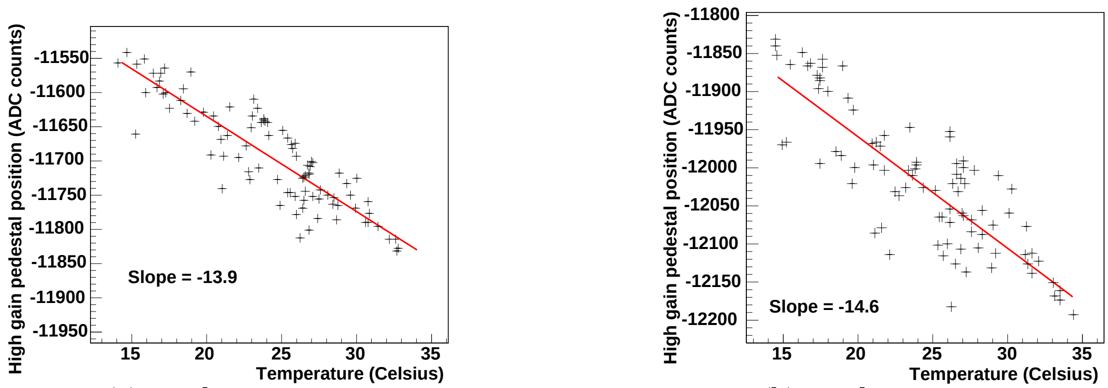

(a) Pixel CT3-E3-05

(b) Pixel CT3-F8-11

Figure 22: Evolution of the high-gain pedestal as a function of the temperature: the correlation is linear and the dispersion around the mean correlation is less than 100 ADC counts, i.e. 1.6 photo-electrons (from March to August 2003).

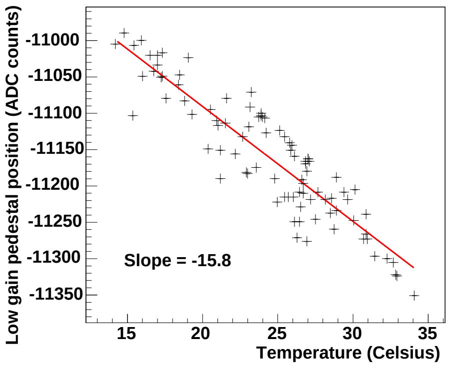

(a) Pixel CT3-E3-05.

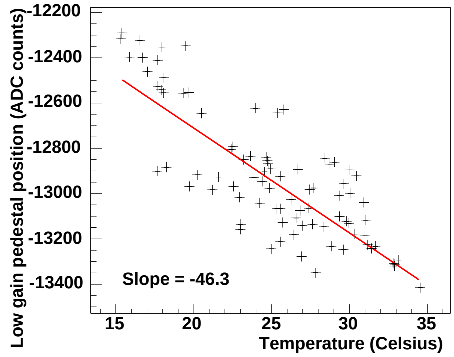

(b) Pixel CT3-A3-00.

Figure 23: Evolution of the low-gain pedestal as a function of the temperature: the correlation is linear and the dispersion around the mean correlation is less than 100 ADC counts, i.e. 1.5 photo-electrons (from March to August 2003).

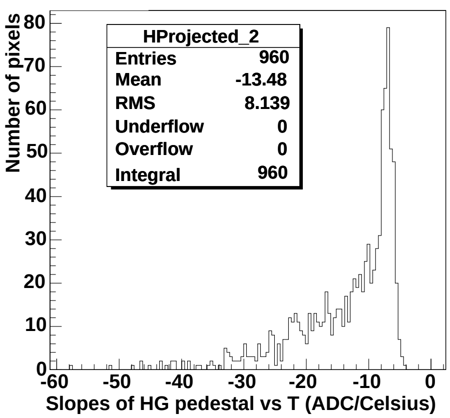

(a) high-gain channels.

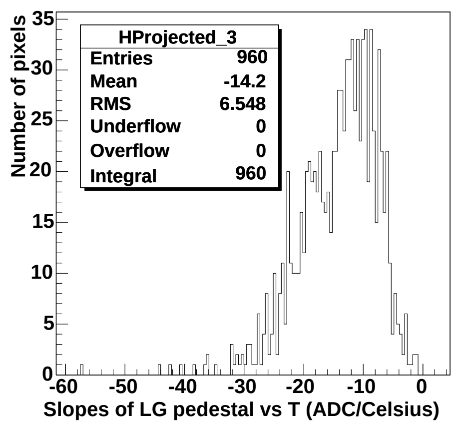

(b) low-gain channels.

Figure 24: Distribution of the slopes of the linear correlations of the pedestal positions with the temperature (from March to August 2003).

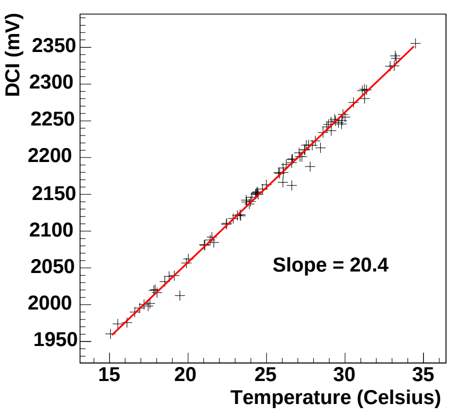

(a) DCI as a function of the temperature (pixel CT3-C6-11).

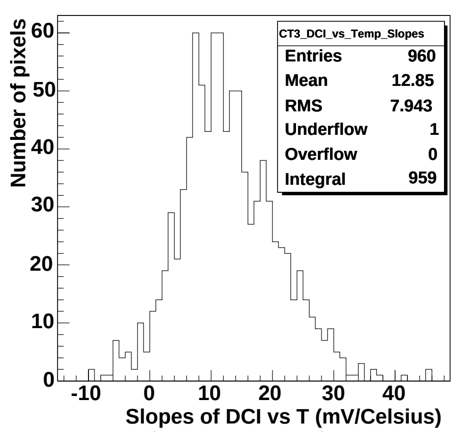

(b) Distribution of the slopes of the correlations.

Figure 25: Evolution of the DCI with the temperature (from March to August 2003).

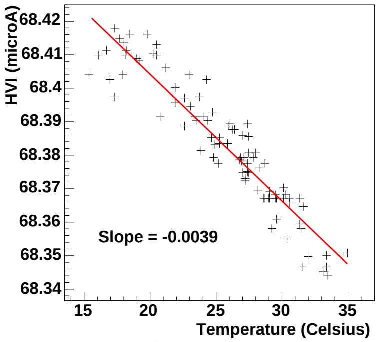

(a) Pixel CT3-D5-14.

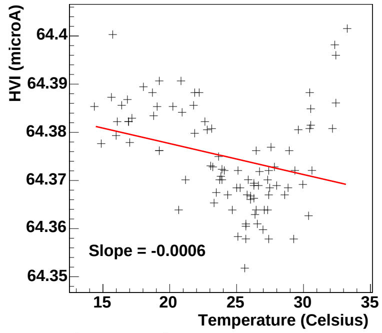

(b) Pixel CT3-C4-04.

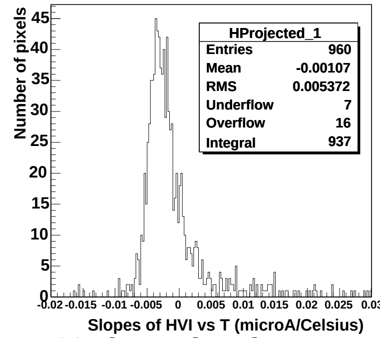

(c) Slopes distribution.

Figure 26: Evolution of the HVI with the temperature (from March to August 2003).

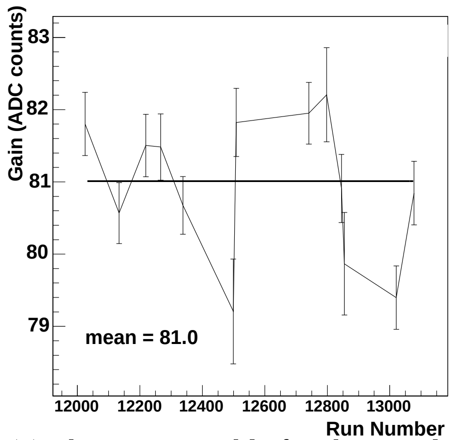

(a) The gain is stable for this pixel.

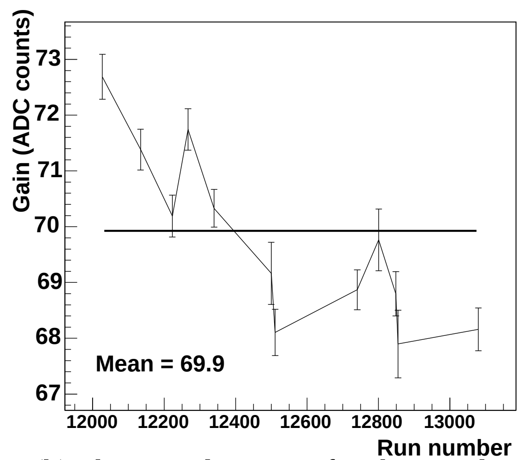

(b) The gain decreases for this pixel.

Figure 27: Evolution of the gain as function of the time: a 3 week shift period.

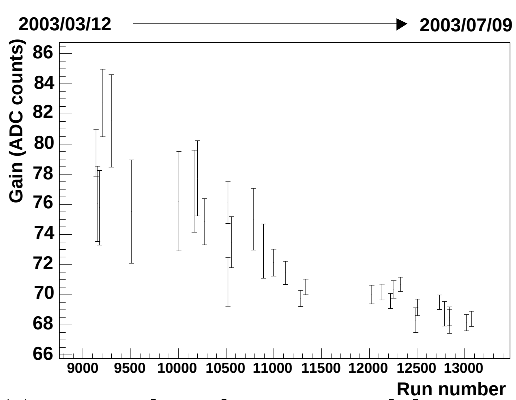

(a) A typical pixel: exponential decrease.

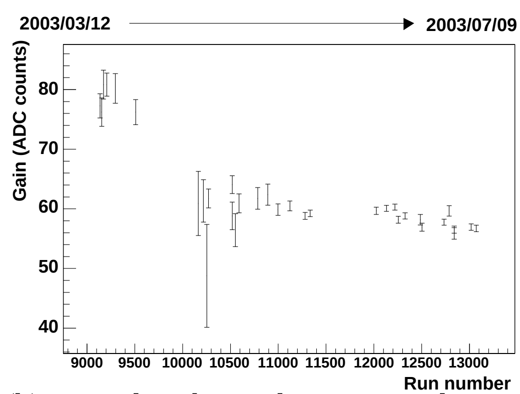

(b) A pixel with an edge in its evolution.

Figure 28: Evolution of the gain for typical pixels over 4 months (March to July 2003).

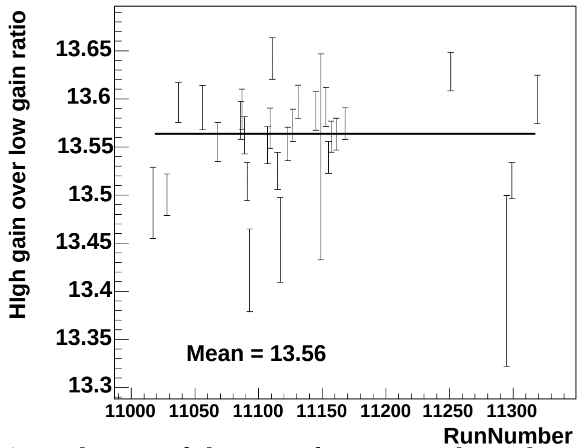

(a) Evolution of the ratio for a typical pixel: it is stable.

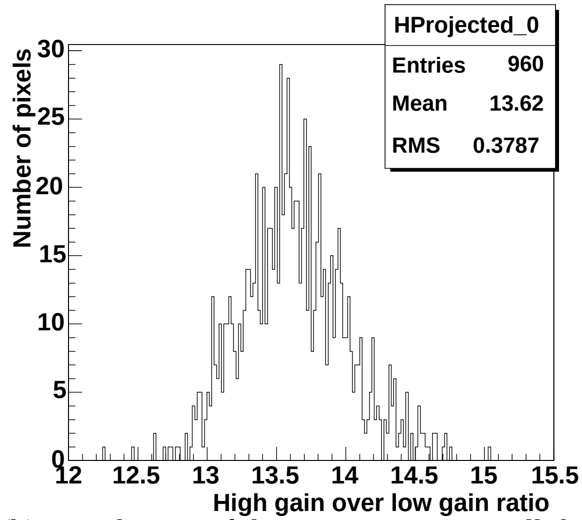

(b) Distribution of the mean ratios over all the pixels.

Figure 29: high-gain to low-gain ratio evolution with time: a 3 week shift period.

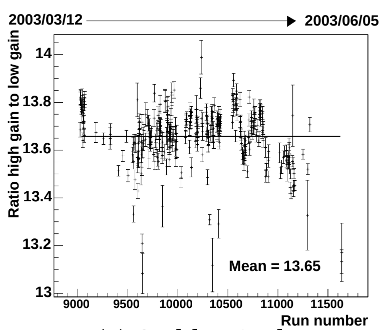

(a) Stable pixel.

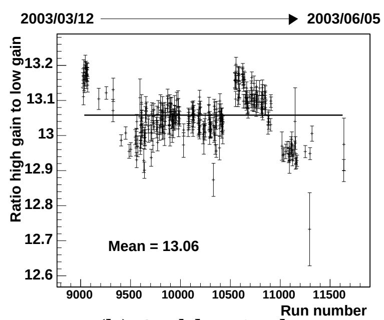

(b) Stable pixel.

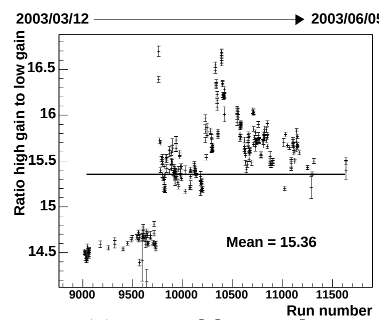

(c) Unstable pixel.

Figure 30: Examples of the evolution of the high to low-gain ratio with time (March to July 2003).

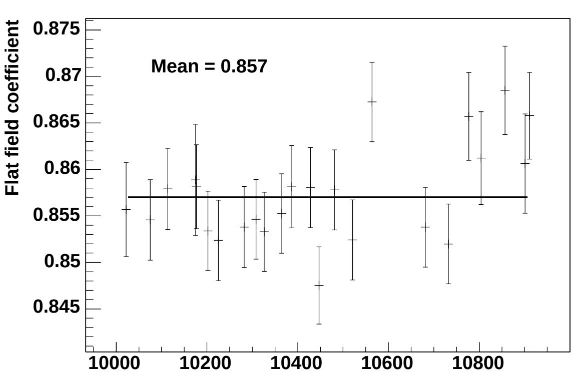

(a) Evolution of the coefficient for a typical pixel (CT3-F6-01): it is stable.

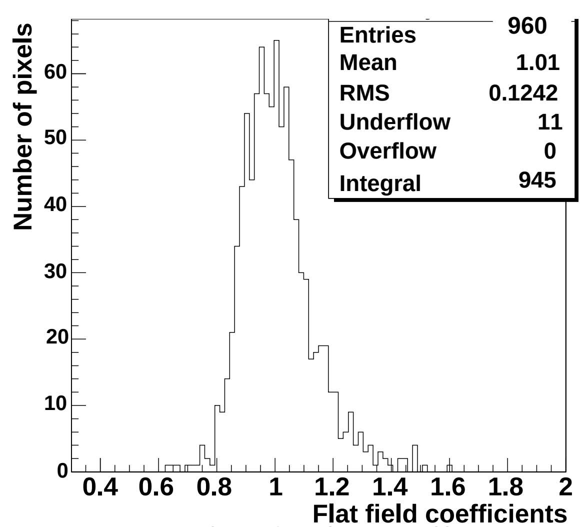

(b) Distribution of the flat-field coefficients in the camera (CT3).

Figure 31: Flat-field coefficient evolution with time: a 3 week shift period (period 2003_04).

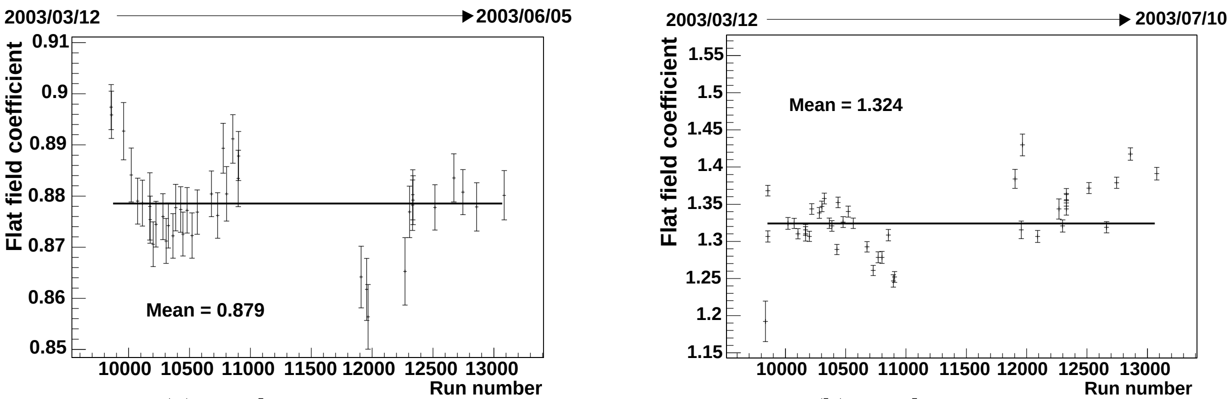

(a) Pixel CT3-E5-05. (b) Pixel CT3-A5-05.

Figure 32: Examples of the flat-field coefficient evolution (March to July 2003).

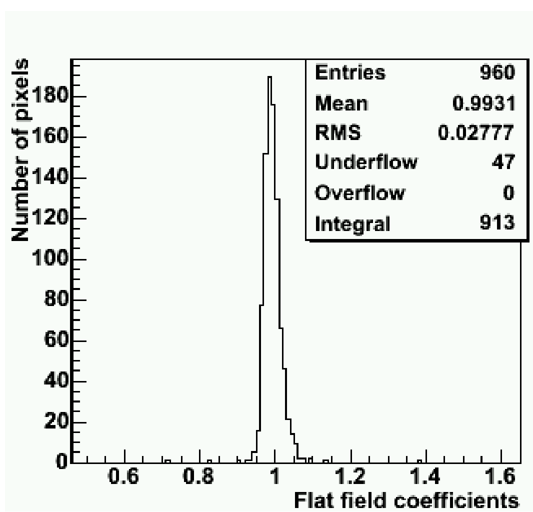

Figure 33: Flat-field coefficients distribution when the flat-field correction is used to compute them again (run 10912). This distribution must be compared to the distribution without flat-field correction figure 20-(c).

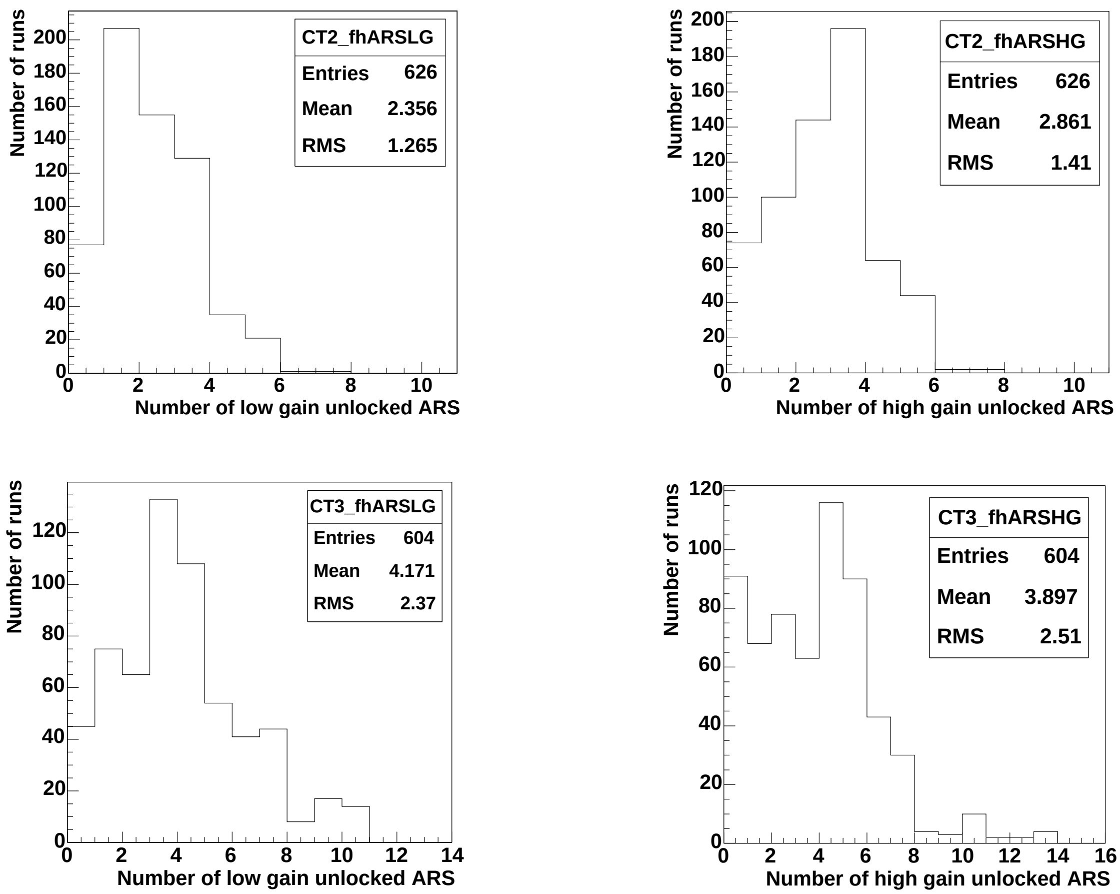

Figure 34: Distributions of the number of unlocked ARS per run (from 25 / 03 / 2003 until 10 / 07 / 2003).

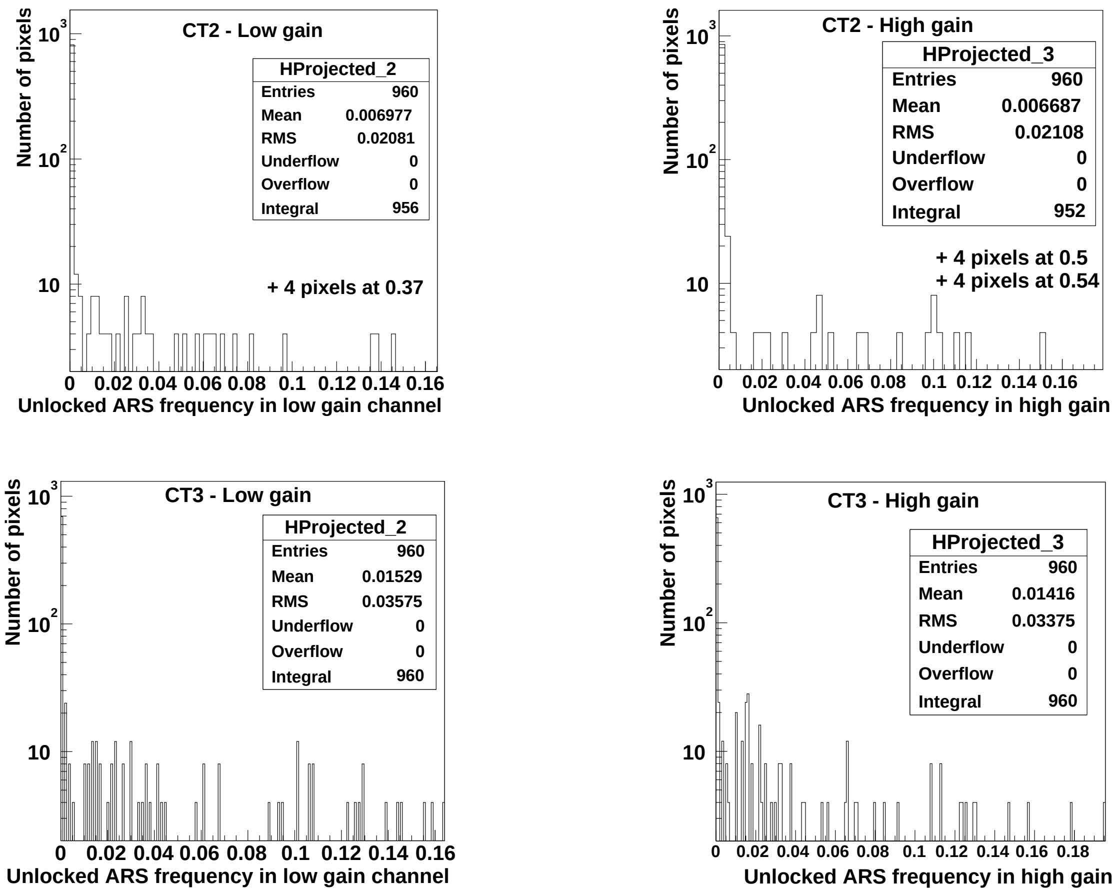

Figure 35: Distribution of the unlocked ARS pixel frequency (from 25/03/2003 until 10/07/2003).

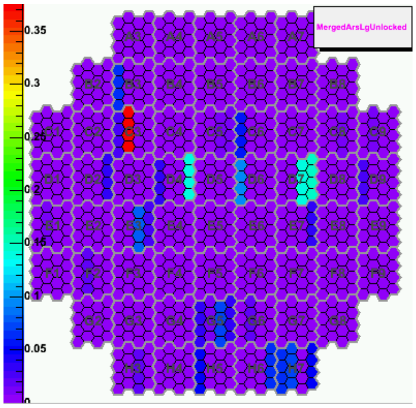

CT2 - Low gain

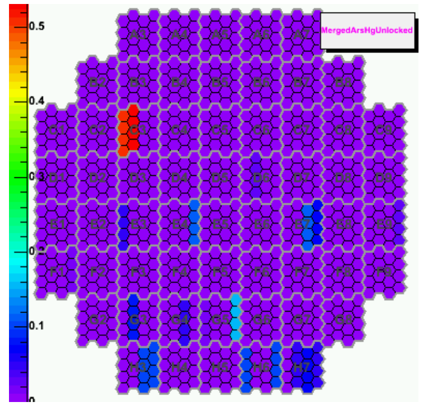

CT2 - high gain

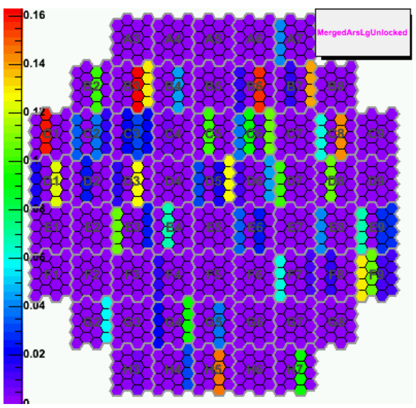

CT3 - Low gain

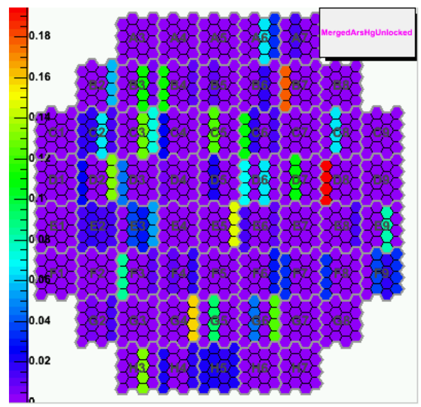

CT3 - high gain

Figure 36: Distribution on the camera of the unlocked ARS pixel frequency.

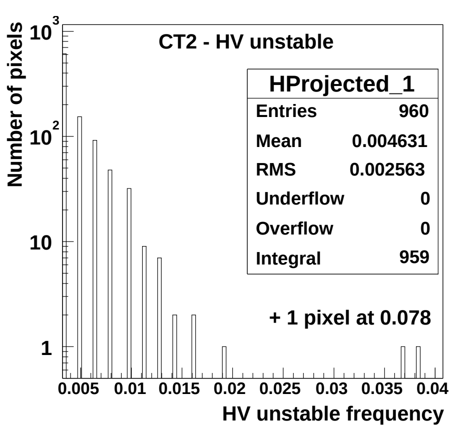

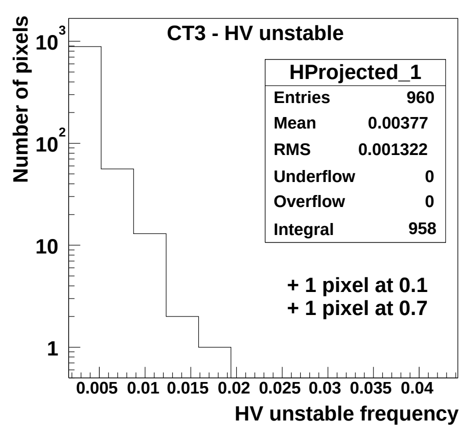

Figure 37: Distribution of the unstable HV pixel frequency (from 25/03/2003 until 10/07/2003).

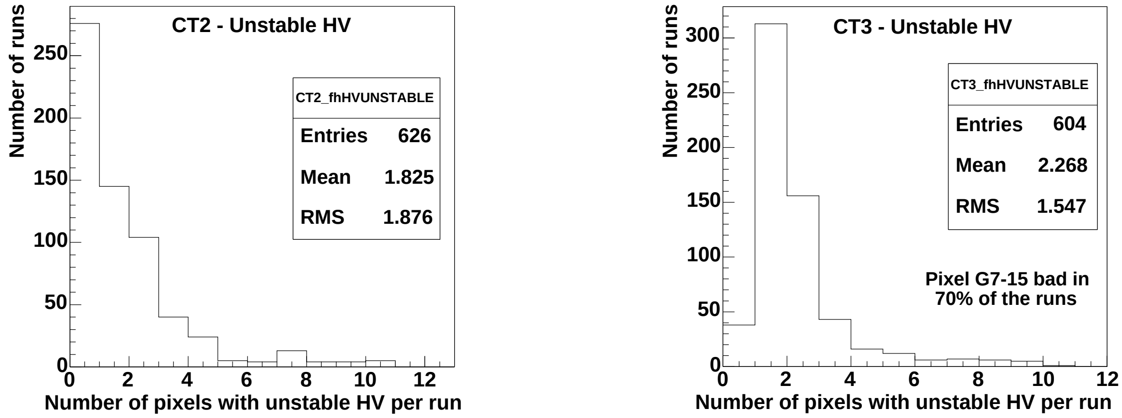

Figure 38: (Distribution of the number of pixels with unstable HV per run (from 25/03/2003 until 10/07/2003).

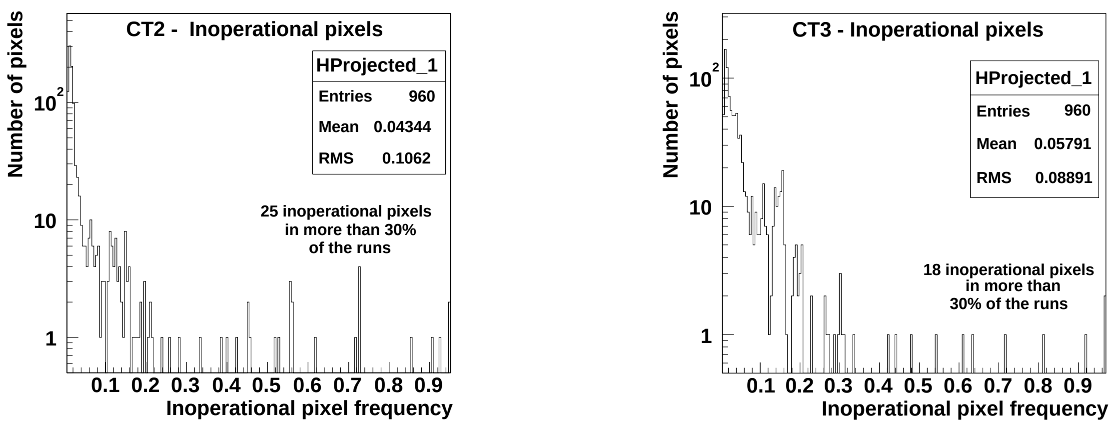

Figure 39: Distribution of the frequencies the pixels are found non-operational (from 25/03/2003 until 10/07/2003).

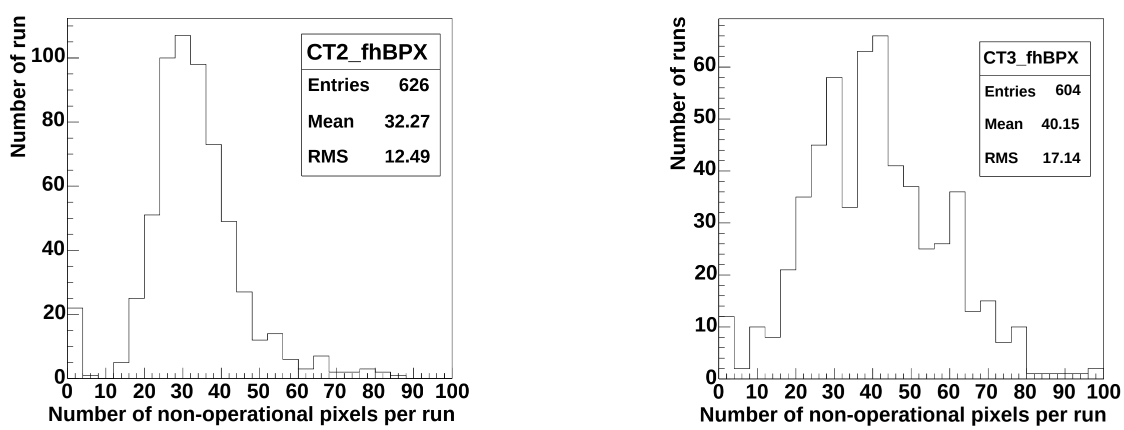

Figure 40: Distribution of the number of non-operational pixels per run (from 25/03/2003 until 10/07/2003).

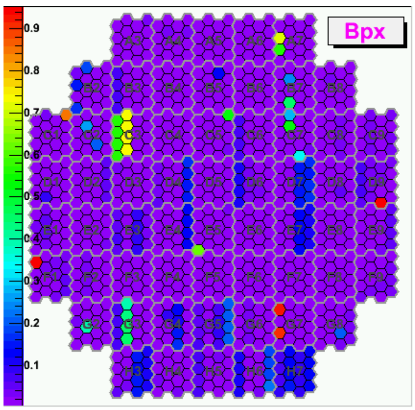

CT2

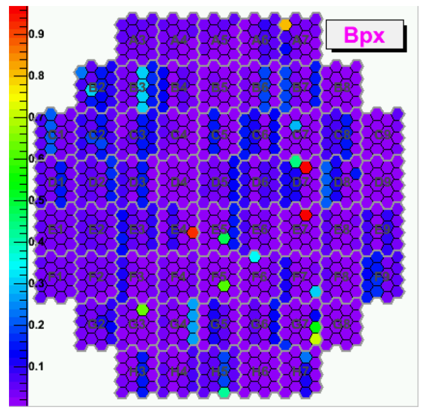

CT3

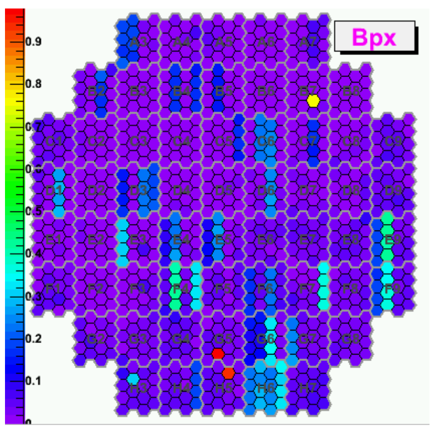

CT4- September 2003

Figure 41: Distribution of the non-operational pixels in the cameras (from 25/03/2003 until 10/07/2003).

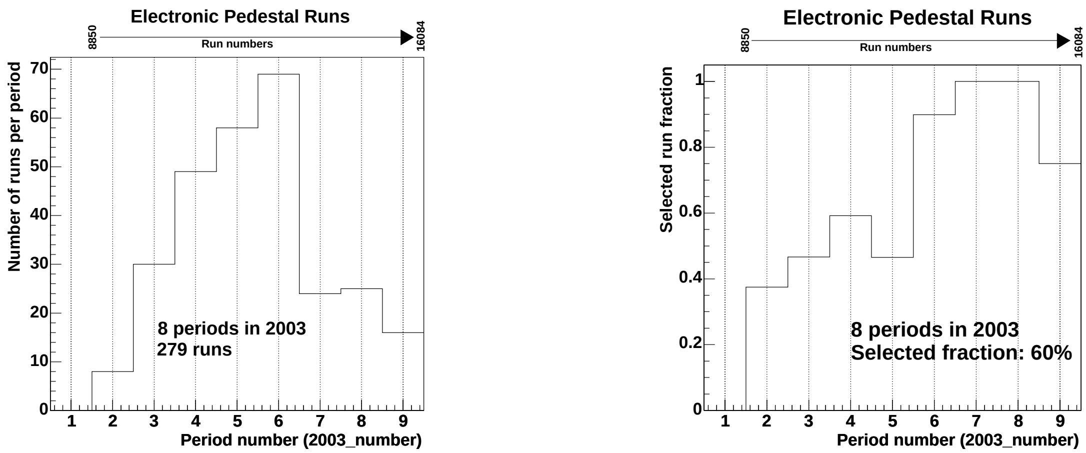

Figure 42: Number of ElectronicPedestalRuns per shift period (from 2003_02 to 2003_09), and fraction of them used in the calibration.

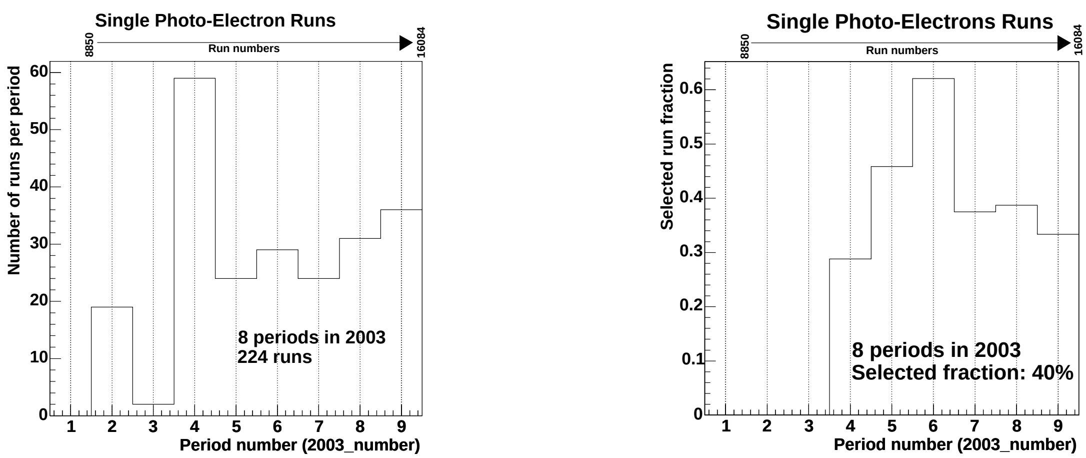

Figure 43: Number of SinglePhotoElectronRuns per shift period (from 2003_02 to 2003_09), and fraction of them used in the calibration.

ANNEXE 1

Names of the 12 tables of the database CALIBRATION used for the classical calibration

- Pedestal_RunQuality
- Pedestal
- Period_Pedestal
- SinglePE_RunQuality
- PMTGain
- Period_PMTGain
- HighLowRatio
- Period_HighLowRatio
- FlatField_RunQuality
- FlatField
- Period_FlatField
- BrokenPixel

References

[1] Tavernet, J.P., HESS internal note (may 2002): “Results from the HESS drawer test bench”

[2] Leroy, N., HESS internal note (april 2003): “Pedestal an NSB determination”

[3] web site of the calibration in Paris: http://lpnp90.in2p3.fr/~hess/calibration/

[4] Redondo,I., HESS meeting, November 2002, transparencies on the unlocked ARS: http://www-eep.physik.hu-berlin.de/hess/protected/meeting/november02/redondo2711.ps

[5] http://www.mpi-hd.mpg.de/hfm/HESS/intern/hess_internal.htm : Manuals/Calibration Instructions